

# Magnesium-Related Donors in Silicon: State of the Art

Yuri A. Astrov,\* Leonid M. Portsel, Valentina B. Shuman, Anatoly N. Lodygin, and Nikolay V. Abrosimov

The research interest in deep donors in silicon is due in particular to the quantum structure of such centers; these are promising for application in silicon photonics in the mid-IR range and quantum technologies. At interstitial lattice positions, magnesium atoms create double-charge deep donors. The review is an attempt to summarize the accumulated knowledge on properties of magnesium impurity in silicon. Among methods to obtain magnesium-doped silicon, there is focus on the impurity diffusion from the solid phase using the so-called sandwich method. Techniques to investigate samples include Hall effect measurements, optical absorption, luminescence spectroscopy, and others. The diffusivity of magnesium in silicon and stability of parameters of doped samples under heat treatment is discussed. The energy spectrum of the helium-like magnesium donor is considered in detail. Due to the interaction with other impurities, magnesium forms a variety of donor levels in silicon. These include complexes of Mg with substitutional acceptor atoms B, Al, Ga, In, interstitial Li, and oxygen, as well as numerous donors with a currently unknown nature. Some defects are similar to so-called thermal donors in silicon. The pairing of Mg atoms is proved in samples prepared from the isotope  $^{28}\text{Si}$ -enriched silicon.

## 1. Introduction

The electronic and optical properties of a semiconductor are largely determined by defects in the crystal lattice. This has led to an ongoing research interest in this area, e.g., recent topical issues “Defects in Semiconductors,”<sup>[1,2]</sup> as well as a review article,<sup>[3]</sup> devoted to a possible application of silicon donor states in the design of quantum computing platforms. However, with regard to silicon, researchers have historically focused on impurities releasing one electron/hole into the conductivity/valence band. Such impurities are specified by relatively low ionization energies, typically in the range of 40–50 meV (these are so called shallow impurities), thus providing large extrinsic conductivity of silicon at room temperature. Up to the present, such shallow centers have been fairly well studied and extensively applied in the

electronic industry. Photonics-related investigations reveal possibilities for far-infrared stimulated emission based on intracenter population inversion and resonant Raman scattering at shallow, single-electron impurities.<sup>[4–7]</sup>

Atoms that donate two electrons or holes into a silicon crystal are characterized by essentially stronger localizations of the ground state and a larger activation energy when compared to those for shallow centers. Impurities with an ionization energy exceeding  $\approx 0.1$  eV are traditionally called deep centers.

The impurity-related electrical and optical properties of Si:Mg are mainly due to the placement of Mg atoms at interstitial ( $\text{Mg}_i$ ) positions in the lattice.<sup>[8–10]</sup> Unlike other elements of the II-group—beryllium<sup>[11]</sup> and zinc,<sup>[12]</sup> which are substitutional acceptors—magnesium forms double donors with a binding energy of electron of  $\approx 107$  meV for the neutral


$\text{Mg}_i^0$  and  $\approx 256$  meV for the singly ionized  $\text{Mg}_i^+$  states, respectively.<sup>[8,9]</sup> (Note that germanium doped with magnesium demonstrates conductivity of  $p$ -type.<sup>[13]</sup>) The intermediate electron binding energy of  $\text{Mg}_i$  between shallow centers and deep chalcogen donors ( $\approx 318$ , 307, and 199 meV for atoms S, Se, and Te in the substitutional positions, respectively,<sup>[14]</sup>) makes magnesium an interesting impurity in silicon from the perspective of the potential application of Si:Mg in mid-infrared (MIR). A method to increase the efficiency of silicon-based solar cells by introducing magnesium into the semiconductor is also discussed.<sup>[15]</sup>

The chemical activity of magnesium and high mobility of interstitial Mg assumes its ability to form complexes by paring with various chemical elements and other defects in the silicon lattice, even at a relatively low temperature. However, these properties of the interstitial Mg impurity may result in changing parameters of Si:Mg on the long-term time scale.

Since the first publication on Si:Mg,<sup>[8]</sup> more than 40 articles have been published on the related topic. However, many properties of magnesium-related impurities in silicon did not receive warranted attention, mainly because of a lack of reliable/reproducible technology and the absence of a sufficiently broad spectrum of research-grade Si:Mg crystals available for studies. Therefore, until recently, there has been no data on some critical parameters for the Si:Mg technology—such as the diffusivity of magnesium in silicon and the thermal stability of the doped material. For the potential application of Si:Mg in the MIR silicon photonics, it is important to have information on fine details of

Y. A. Astrov, L. M. Portsel, V. B. Shuman, A. N. Lodygin  
 Ioffe Institute  
 Russian Academy of Sciences  
 Politekhnikeskaya 26, 194021 St. Petersburg, Russia  
 E-mail: yuri.astrov@mail.ioffe.ru

N. V. Abrosimov  
 Leibniz-Institut für Kristallzüchtung (IKZ)  
 Max-Born-Straße 2, 12489 Berlin, Germany

 The ORCID identification number(s) for the author(s) of this article can be found under <https://doi.org/10.1002/pssa.202200463>.

DOI: 10.1002/pssa.202200463

the energy structure of Mg-related donors, as well as data on the spatial localization of the ground and excited states of centers. There have been few detailed studies on Mg-related complexes. The dependencies of the concentration of Mg in its electrically active state and those electrically inactive magnesium on the doping conditions and post-doping treatment of crystals were not known at the required level of detail. Some relevant recent results are discussed in the article.

Different approaches to the doping silicon with magnesium are reviewed in the article and are based on doping during crystal growth, from the gas phase, in the course of the epitaxial growth of a Si:Mg film, or by ion implantation followed by a thermal annealing of a sample. Finally, the diffusion of Mg from the solid phase by the so-called sandwich method that was described and employed in the very first work in the field,<sup>[8]</sup> turned out to be the most productive so far, and has been further developed. Basic information on the properties of Si:Mg crystals has been obtained for samples doped with this technique.

In recent years, there has been a systematic study into the doping of the research-grade silicon with magnesium alone and in diverse combinations with other elements. As a consequence, high-quality Si:Mg crystals have become available for the research. Some previous results have been revisited, renewed, and extended, while new findings have revealed unexpected properties of magnesium-related donor centers. In particular, many new results have been obtained using the highly purified and isotopically enriched silicon lattices by the analysis of low-temperature infrared absorption spectroscopy—including spectroscopy in strong magnetic fields and under uniaxial deformation of Si:Mg crystals, as well as by observing impurity-related photoluminescence.

## 2. Review of Doping Techniques

For a possible application in silicon photonics, it is sufficient (and sometimes even optimal) to have a rather low concentration of active impurity, typically in the range of  $10^{15}$ – $10^{16}$  cm<sup>−3</sup>.<sup>[4,5,16]</sup> At these concentrations, the impurity–impurity interaction is relatively weak; thus, the electronic structure of the impurity subsystem is essentially the same as that for individual localized centers. This chapter summarizes methods that have been proposed to prepare Si:Mg crystals, and, which thus could be potentially applied to obtain the required concentrations of magnesium double donors.

### 2.1. Doping in the Course of Crystal Growth from the Melt

The doping of semiconductors with electrically active impurities in the course of a crystal growth from the melt is among standard techniques employed in the electronics industry. The application of this technology to obtain Si:Mg samples is difficult because of a high magnesium vapor pressure at the crystallization temperature of silicon, as well as owing to the low segregation coefficient of Mg in Si. Nevertheless, such attempts were made in refs. [17,18] where a crucible-free pedestal method was used.

To suppress the rapid evaporation of magnesium, which occurs when an Mg pill is added directly into the melt, the pill is placed into an axial hole on the top of a polycrystalline or

float-zone (FZ) grown high-purity Si feed rod that is always covered with the melt. Thus, the growth begins with pure Si, and the dopant gradually evaporates with increasing temperature at the base of the hole, moving down the melting boundary during the crystal growth. Thus, the melt zone is steadily saturated with magnesium. This technique enables an active Mg<sub>i</sub><sup>0</sup> donor concentration of up to  $5 \times 10^{14}$  cm<sup>−3</sup> to be obtained in samples, as estimated from the intensity of Mg<sub>i</sub><sup>0</sup> transitions in the infrared absorption spectra.<sup>[18]</sup> However, the described method is rather complicated and has not been subsequently used.

### 2.2. Gas-Phase Doping

Gas-phase doping is widely used in silicon device technology. When applying the method to prepare Si:Mg samples, flakes of metallic Mg can be placed together with the initial Si wafers in an enclosed volume. A sealed quartz ampoule can be used to conduct the diffusion process at a temperature that provides high magnesium vapor pressure. However, magnesium vapor reacts with quartz according to the reaction



As a result, the diffusion source is quickly exhausted, thus making it challenging to obtain a high concentration of Mg in a sample. Nevertheless, attempts to use the method for the preparation of Si:Mg samples were reported in refs. [19–21]. As mentioned in ref. [19], the concentration of magnesium of  $\approx 1.2 \cdot 10^{14}$  cm<sup>−3</sup> was obtained in samples using the discussed method.

In ref. [20], Mg with a purity of 99.9% was used. According to the Hall effect data, two types of impurity states were observed in doped crystals: The first one was amphoteric, thus exhibiting both acceptor and donor properties. The second impurity state corresponded to a donor level. The physical nature of these Mg-related centers was not clarified in the cited work. However, activation energies for all observed centers did not correspond to the data obtained by the optical spectroscopy of ref. [8]. The results of the study,<sup>[21]</sup> which also reported the observation of an amphoteric state of impurity in Si:Mg, are outlined in Section 3.5.

In another study of the diffusion doping from a gas phase,<sup>[22]</sup> MgB<sub>2</sub>–MgO composite was used as a source of the magnesium vapor. The purity of Mg in the experiments was 99.9%. The composite was put in an alumina crucible, while a Si wafer was placed above it. At a high temperature, MgB<sub>2</sub> was decomposed into Mg and MgB<sub>4</sub>. Thus, the magnesium vapor served to dope the wafer. Processing of samples for 2 h at 1000 °C, a p<sup>+</sup>-layer with a thickness of  $\approx 6$  μm on a sample surface was observed, the hole concentration in the layer being  $\approx 10^{21}$  cm<sup>−3</sup>. According to the authors' interpretation of data, the high concentration of acceptors in the layer was a result of the fact that Mg atoms were in the substitution positions; here—similar to Zn and Be—they could serve as acceptors. However, the high surface concentration of acceptors in the sample and the low diffusion coefficient of the impurity could indicate the diffusion of boron in the experiment, rather than of magnesium.

### 2.3. Liquid-Phase Epitaxy from Mg/Si Melt

In ref. [23], a sandwich epitaxy method was applied to dope silicon with magnesium as follows. First, the silicide  $\text{Mg}_2\text{Si}$  layer was grown on a silicon surface through the reaction of magnesium vapor with silicon. A typical thickness of obtained silicide layers was in the range of 10–20  $\mu\text{m}$ . Next, the grown layer was covered by another silicon wafer. This structure was then placed in a vertical furnace filled with argon, where a temperature gradient perpendicular to the sample surface was set. At a selected epitaxy temperature, the magnesium-doped silicon layer grew toward the cooler side of the sandwich. Data on the temperature dependence of magnesium solubility in silicon were obtained by measuring the impurity concentration in the samples using flameless atomic absorption spectroscopy. Its value reached  $\approx 10^{19} \text{ cm}^{-3}$  at 1200 °C.

Doping silicon with magnesium by employing the epitaxy method has also been performed in a recent work,<sup>[24]</sup> where Si:Mg layers of a thickness  $\geq 160 \mu\text{m}$  were obtained in the temperature range of 1050–1350 °C. The Mg content in the layers was determined by using an electron probe analyzer. Compared to data reported in ref. [23], the solubility of Mg in Si was an order of magnitude lower. The authors interpreted this discrepancy assuming that the samples studied in ref. [23] included metallic magnesium (Mg clusters), which significantly contributed to the recorded content of the impurity, thereby overestimating the value of its solubility.

### 2.4. Ion Implantation

The doping of semiconductors by ion implantation is widely used in technology. The method was applied in ref. [25] to dope Si with Mg. Magnesium ions with energy in the range of 80–150 keV and doses of  $5.0 \times 10^{14}$  and  $5.0 \times 10^{15} \text{ cm}^{-2}$  were implanted into *p*-type silicon wafers, which had a resistivity of 50  $\Omega \text{ cm}$ . After annealing of samples, profiles of the total magnesium concentration over a layer depth—where the crystal structure had been damaged during implantation—were measured by the mass-spectroscopy of secondary ions (SIMS). In the same area of the sample, the concentration of electrically active centers was defined using the Hall effect measurements (to find the depth profile in the concentration of electrons, the anodic stripping technique was used). It was found that the total concentration of magnesium in the sample significantly exceeded—by several orders of magnitude—the concentration of electrically active impurity, which confirmed the results of the previous work,<sup>[23]</sup> where samples were doped with the liquid-phase epitaxy. To interpret these observations, the authors advanced the hypothesis that the impurity was mainly in the form of neutral isoelectronic pairs that formed owing to coupling interstitial and substitutional Mg atoms. It was also proposed that only a small part of magnesium atoms occupied interstitial positions in the crystal lattice, thus providing the electrical activity of the impurity. In the same work, another interesting fact was noted: upon prolonged annealing of the doped layers, the concentration of electrically active magnesium Mg<sub>i</sub> decreased (and this process was irreversible), while for other impurities in silicon, it is usually known to increase.

Thus, to obtain a significant content of electrically active magnesium in a sample, the total dose of implantation has to be sufficiently high. From the data reported in ref. [25], it follows, for example, that the sheet concentration of electrically active magnesium  $\approx 3.0 \times 10^{12} \text{ cm}^{-2}$  could be achieved by irradiation with a dose of  $5.0 \times 10^{15} \text{ cm}^{-2}$  and subsequent heat treatment. The effect of annealing of ion-implanted samples on the spatial distributions of the total density of magnesium was also studied in ref. [26].

With respect to ion implantation methods, it is appropriate to mention the ref. [27], where the natural doping of silicon wafers with magnesium in open space was observed. The effect was due to the irradiation of a wafer by the high-energy magnesium ions, which are a part of the solar wind.

A method called “laser implantation” of magnesium in a sample was proposed in ref. [28]. It included the deposition of a 0.2  $\mu\text{m}$  Mg layer on a high-resistance *p*-Si, which was followed by the subsequent irradiation of the surface with a high-power laser. Finally, the sample was annealed at 1200 °C for 10 h. As a result, an *n*-type layer with a thickness of  $\approx 610 \mu\text{m}$  was obtained on the sample surface. The results published in the study can be used to estimate the diffusion coefficient of the doping impurity. For a given thickness of the doped layer and duration of the annealing, such an estimate gives a rather low diffusivity value of  $\approx 10^{-10} \text{ cm}^2 \text{ s}^{-1}$ . Such a result contradicts the data obtained at the systematic study of the magnesium diffusivity in silicon,<sup>[29–31]</sup> see Section 3.2. Therefore, it appears that the effect observed in ref. [28] was due to the doping of crystals by some other (slowly diffusing) impurity.

Summarizing the described doping methods, the following can be noted: 1) These technologies did not lead to the development of a method suitable for preparing high-quality samples doped by electrically active magnesium, which are required for a comprehensive study of this material. The problems of doping silicon with magnesium are particularly associated with the high volatility of Mg, even at relatively low temperatures. 2) The doping techniques should avoid the concomitant sources of dopants that can contribute to the appearance of unwanted electrically active centers, which also includes Mg-related complexes. This requirement refers both to the purity of magnesium (commercially available up to 99.995%) and to materials in the environment “contacting” a Si crystal in the course of a high-temperature doping process. 3) Not all of the above discussed technologies were supported by a proper analysis of obtained samples. In particular, this refers to the lack of the optical spectroscopy of electrically active centers in obtained samples.

Progress in the technology of Si:Mg has been mainly achieved by applying the diffusion doping from a solid phase—the so-called sandwich method.

## 3. Sandwich Method: Technology and Characterization of Samples

The application of the sandwich method to dope silicon with magnesium was first proposed in ref. [8]. The sandwich was formed by two silicon wafers contacting each other through a layer of magnesium, which was prepared by an evaporation of the metal in vacuum. The initial silicon was of the *p*-type with

a resistivity of  $\rho = 2 \times 10^3 \Omega \text{ cm}$ . Diffusion was accomplished in a helium atmosphere at  $T = 1350^\circ \text{C}$  for 30 min. As a result, the conductivity of samples changed from *p*- to *n*-type, while their resistivity became  $\approx 5 \Omega \text{ cm}$ . Studies of absorption spectra of samples carried out in the temperature range 15–200 K showed that the magnesium impurity in silicon was a double donor whose ionization energies for the neutral ( $\text{Mg}^0$ ) and singly charged ( $\text{Mg}^+$ ) states were 106.8 and 253.4 meV, respectively. It was also found that the excited states of  $\text{Mg}^0$  and  $\text{Mg}^+$  correspond to helium-like series for neutral and singly charged centers. The authors also concluded that the optical activity of the impurity was due to magnesium atoms at interstitial positions in the lattice.

We note that the Si:Mg samples were prepared in the cited work with a continuous gas flow inside the reactor. However, the doping could also be performed in a closed quartz ampoule, see, e.g. [9,10,32–34]. The use of the sandwich method enabled the preparation of Si:Mg crystals with a concentration of optically active interstitial centers of Mg, reaching  $1.5 \times 10^{15} \text{ cm}^{-3}$ . The technology was then applied to investigate energy spectra of Mg centers, including sophisticated methods such as piezo- and magneto-optical studies, see refs. [9,33] and to develop infrared (IR) photoelectric detectors. [35]

The following sections of the review are devoted to results obtained when studying Si:Mg prepared by the sandwich method. It is demonstrated that a proper implementation of the sandwich technology and the use of the high-purity magnesium makes it possible to obtain uniformly doped samples with dimensions that are required to carry out both optical and various kinds of electrical measurements.

### 3.1. Technical Details of Doping

To proceed with the investigation of silicon doped with magnesium, we have revisited the sandwich method. The technology was applied to prepare a variety of bulk-doped samples—both doped only with magnesium, and in combinations with other impurities. Among the important stages of the work, several that are critical for the diffusion doping technology parameters—such as the diffusion coefficient of magnesium in silicon, and technological regimes required to obtain homogeneously doped samples with a high density of electrically active magnesium—were determined.

The initial silicon wafers in our study were usually research-grade dislocation-free *p*- and *n*-type silicon crystals with a diameter of 10–30 mm and a thickness of 0.4–3 mm. Most of the research was carried out using the FZ Si grown at the Leibniz-Institut für Kristallzüchtung (IKZ, Berlin). In particular, this concerned the high-purity silicon with a low concentration of oxygen and carbon, *p*-Si doped with shallow acceptors (B, Al, Ga, In), enriched ( $^{28}\text{Si}$ ) material—both of the high purity and the boron doped. Some samples were prepared using commercial FZ silicon as an initial material. When describing experimental data, the type of material used is mentioned, and the specific resistivity is given.

After a standard sequence of wafer cleaning operations, an Mg film was deposited to one or both of its sides by evaporating the metal in a vacuum of  $\approx 10^{-6}$  Torr. The wafer had either ground or

polished surfaces. Magnesium with a purity of up to 99.999% supplied by Goodfellow GmbH, and MaTeCK GmbH was used as a source of diffusion. In experiments where the diffusion profiles of the impurity were studied, the magnesium layer was deposited only on one side of the wafer, see Section 3.2.

Wafers' surfaces plated with Mg layers were covered with auxiliary silicon plates with a thickness of approximately 0.5 mm. A prepared sandwich was housed into a quartz cartridge and secured there with silicon wedges, as shown in Figure 1. An ampoule was then filled with argon, with the estimated gas pressure at the diffusion temperature being  $\approx 1 \text{ atm}$ , and it was then sealed.

Diffusion doping was performed in the temperature range of 1000–1250  $^\circ\text{C}$  and for a time ranging from 0.5 to 22.5 h. After the diffusion, an ampoule was usually cooled with a jet of compressed nitrogen or air. The typical time required for cooling a sample to a temperature at which the visible glow of silicon disappeared was  $\approx 10^2 \text{ s}$ . Some experiments were performed on samples rapidly quenched after diffusion. In such cases, an ampoule with a sample, which had a diameter of  $\approx 10 \text{ mm}$ , was cooled in a mineral oil.

From the results of the high-temperature diffusion process, the auxiliary plates and the sample became welded to each other. The material of auxiliary plates was then removed by sample grinding. The concentration of Mg<sub>i</sub> in doped samples may reach  $2 \times 10^{15} \text{ cm}^{-3}$ . It should be noted that the slow cooling of the samples together with the furnace led to a decrease in the concentration of electrically active magnesium by about two orders of magnitude. This estimate follows from the results of doping FZ *p*-Si (boron concentration  $N_B = 3 \times 10^{13} \text{ cm}^{-3}$ ) with magnesium. In case of the slow cooling after diffusion, the samples remained of *p*-type. That is, concentration of the double donor in them did not exceed  $1.5 \times 10^{13} \text{ cm}^{-3}$ . This result is evidently due to the fact that the decomposition of the solid solution of interstitial magnesium occurs in the course of a slow cooling, see also Section 3.4. In this regard, we also note that the rapid quenching of a sample used in ref. [9] by immersing it in liquid nitrogen did not lead to a noticeable increase in the Mg<sub>i</sub> concentration.

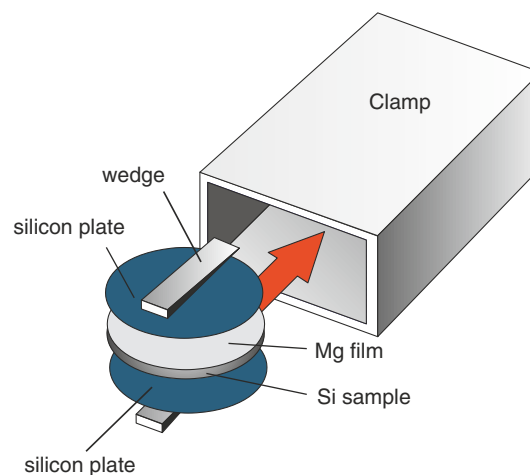


**Figure 1.** Schematics of the insert in an ampoule prepared for diffusion.



The diffusion temperature of magnesium into silicon typically exceeds 1000 °C. At such a high  $T$ , the source of the impurity diffusion is the Mg–Si melt, which is apparently formed in the boundary region of the sandwich, see e.g., the binary phase diagram for these elements in ref. [36]. One may propose that at a transient stage at the temperature increase—where the sandwich is heated from a low temperature—a film of silicide  $\text{Mg}_2\text{Si}$  may form at the interface, see e.g. [37,38]. It was shown [23] that the  $\text{Mg}_2\text{Si}$  layer may serve as a source of magnesium diffusing into the silicon volume; see also ref. [37].

### 3.2. Diffusivity of Magnesium in Silicon

The temperature dependence of diffusivity  $D_{\text{Mgi}}$  for the interstitial magnesium that provides the electrical activity of the impurity in Si was determined in refs. [29–31] see **Figure 2**. The results that are shown refer to a high-purity dislocation-free FZ silicon used as an initial material to diffuse magnesium. For the high-temperature range,  $T = 1000\text{--}1200$  °C, the data were obtained by measuring the depth profiles of interstitial magnesium in doped samples. This was performed using the differential conductivity method. [29,31] In the low-temperature region,  $T = 600\text{--}800$  °C, the  $D_{\text{Mgi}}(T)$  dependence was determined using samples doped by ion implantation. In this case, [30] initial wafers were of the  $p$ -type with a resistivity of 450  $\Omega$  cm. Mg ions with an energy of 150 keV were implanted into the wafers at room temperature at doses of  $F = 5.0 \times 10^{14}$  and  $2.0 \times 10^{15}$   $\text{cm}^{-2}$ . The diffusion coefficient at a given  $T$  was determined by measuring a depth of the  $p$ - $n$  junction formed in a sample by annealing at a time  $t$ .

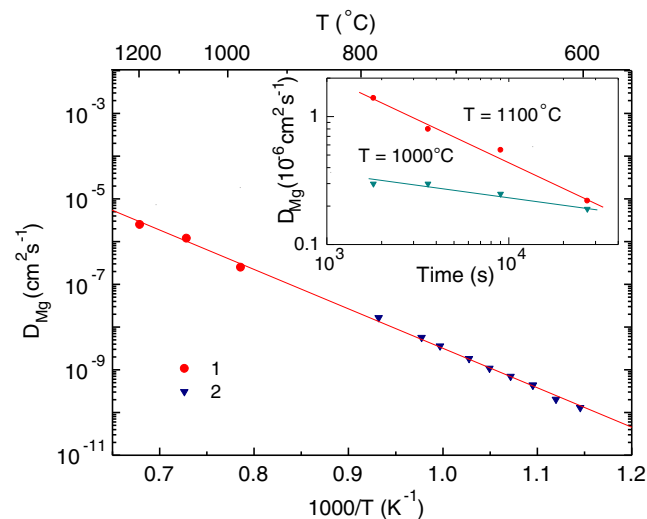


**Figure 2.** Main panel: temperature dependence of the diffusion coefficient of interstitial magnesium at relatively short diffusion times, refs. [29–31]. The data were obtained as follows: 1—measuring the diffusion profiles of impurity concentration in sandwich-doped samples by applying the differential conductivity method; 2—finding depths of  $p$ - $n$  junctions formed as a result of the annealing of samples prepared by doping  $p$ -Si wafers with Mg+ implantation. Adapted with permission. [31] Copyright 2017, Wiley-VCH Verlag. The inset shows the variation in time for the effective magnesium diffusivity at two processing temperatures, as measured by the differential conductivity method. Adapted with permission. [40] Copyright 2020, Pleiades Publishing, Ltd.

In the whole temperature range of 600–1200 °C, the diffusivity was found to be well approximated by the Arrhenius expression [31]

$$D_{\text{Mg}} = (5.3^{+1.0}_{-1.0}) \times \exp\left(-\frac{(1.83 \pm 0.02)\text{eV}}{k_{\text{B}}T}\right) \quad (2)$$

where  $T$  is in K, and  $k_{\text{B}}$  is the Boltzmann constant. The dependence (1) is shown in the main panel of Figure 2 by the solid line.

Note that the temperature dependence of the diffusion coefficient of magnesium (2) found in refs. [29–31] was interpreted in ref. [39] on the basis of a thermodynamic analysis of processes that determine the mobility of magnesium atoms in the silicon lattice.

It was also revealed that the effective diffusion coefficient of  $\text{Mg}_i$  decreases with an increase in the diffusion time, [40] see inset in Figure 2, which shows the corresponding data for two diffusion temperatures. According to the hypothesis proposed in the cited work, the observed effect is associated with the peculiarities of the kinetics of intrinsic defects in the silicon crystal lattice: owing to the interaction of interstitial magnesium with defects, the mobility of  $\text{Mg}_i$  decreases during the diffusion. These preliminary data may indicate that at long diffusion processes carried out at close temperatures, the effective diffusivities of electrically active magnesium tend to be approximately equal. However, the observed effect requires more detailed consideration.

According to experiments reported in ref. [31], a larger diffusion coefficient of electrically active magnesium is observed in silicon containing a high dislocation density: Mg-diffused samples prepared from a FZ Si with a dislocation density of  $5.4 \times 10^3 \text{ cm}^{-2}$  demonstrate the  $D_{\text{Mgi}}$  value that is approximately increased by an order of magnitude compared to a FZ dislocation-free silicon.

One can state that magnesium should be classified as a rapidly diffusing impurity in silicon, as is the case with other elements occupying interstitial positions in the crystal, such as Li, [41] Fe, [42] Cu, [43] and Ni. [44]

#### 3.2.1. On the Total Amount of Magnesium in Mg-Diffused Samples

It has been reported long ago that only a small proportion of magnesium atoms in Si:Mg is in electrically active states. This regularity was observed in samples prepared by two methods—with epitaxy [23] and the ion-implantation [25] techniques, see data presented in Figure 9 and 10 in ref. [25]. As noted in the above references, most of the magnesium content in a doped crystal is in an electrically inactive state. In ref. [25], it was assumed that a large part of this “neutral” magnesium can exist in the form of isoelectronic pairs  $\text{Mg}_i\text{--}\text{Mg}_s$  (where  $\text{Mg}_s$  is a magnesium atom at the substitutional position), clusters of Mg atoms, or inclusions (precipitates) of magnesium silicide  $\text{Mg}_2\text{Si}$ . We mention here that a number of fast diffusing impurities, including Li, Ni, and Cu, can condense in silicon, thus forming precipitates. [45] However, the structure of the neutral component of magnesium in silicon remains unknown up to this point.

A large density of the neutral magnesium was also observed in samples doped with the sandwich method, [40] where impurity

diffusion profiles were investigated. As an initial material, the high-purity *n*-Si was used in the experiments. Profiles of electrically active, as well as of the total, concentrations of magnesium were measured by employing differential conductivity and the SIMS methods, respectively. It was determined that the total concentration of magnesium exceeded that of the electrically active component by  $\approx 2$ –3 orders of magnitude.

A recent study of the low-temperature luminescence of Si:Mg samples has revealed the existence of Mg–Mg pairs,<sup>[46]</sup> which do not appear to be electrically active, see Section 4.4.3 below. In the same work, a number of luminescence lines at different photon energies have been observed, which may indicate the presence in crystals of either magnesium clusters or the precipitates of the dispersed phase of magnesium silicide. One may expect that the formation of magnesium precipitates could lead to an increase in the scattering of free electrons in the conduction band, and accordingly, to a decrease in their mobility. A decrease in the electron mobility in Si:Mg, which was observed in ref. [47], was explained by the authors taking into account the presence of structural micro defects in samples.

We have compared the temperature dependence of electron mobility  $\mu_e(T)$  determined for a commercially available FZ *n*-Si with a low donor concentration ( $\rho = 500 \Omega \text{ cm}$ ) with that measured in samples prepared by doping a high-purity silicon with magnesium. In contrast to results of ref. [47], no noticeable decrease in  $\mu_e$  was observed due to the presence of magnesium. However, it should be emphasized that samples studied in the above cited work were obtained by doping a Czochralski-grown (Cz) silicon (which is characterized by a significant oxygen content). Therefore, our data—where a FZ silicon is used—indicate a low impact of the high density of electrically inactive magnesium impurity on the electron mobility.

### 3.3. Study of Doped Samples with the Hall Effect Measurement

A knowledge of parameters of a sample obtained in a specific technological process provides information for adjusting the doping regimes when necessary. In the case of silicon doped by a shallow impurity (the largest intracenter energy gap  $\approx 250 \text{ K}$ ), its concentration can be directly estimated from resistivity at room temperature ( $\approx 300 \text{ K}$ ). The application of such a technique for silicon doped with deep double donors (the largest intracenter energy gap  $> 520 \text{ K}$ ) is generally invalid because of the helium-like (and therefore possible different charge states) nature of the centers and their large ionization energies. However, the partial concentrations of impurity centers at different charge states can be obtained by examining the temperature-dependent Hall effect. This method was used particularly to determine the content of deep double donors S and Se, see ref. [48] and further references therein.

In ref. [9], there was an unsuccessful attempt to apply the method to impurity states in Si:Mg samples obtained by the sandwich method. As the authors noted, this was due to inhomogeneities in the electrical properties of doped samples. The Hall effect measurements to investigate samples doped with the sandwich method were used in ref. [32], and a variety of levels was found in the samples. Some of them—with a relatively low activation energy—may have been due to magnesium complexes

with unidentified impurities, see also ref. [49]. Their appearance may be due to either an insufficient purity of magnesium used or the contamination of samples at the high temperature of doping.

In ref. [20], the method was applied to study samples prepared by doping from the magnesium gas phase. However, the data on the energy levels of magnesium obtained in studies<sup>[20,32]</sup> did not correspond to results reported in ref. [8], and thus could not provide the quantitative information on the concentration of electrically active magnesium in the samples.

Here, we illustrate an application of the method to determine the electrically active magnesium content in samples.<sup>[31,50,51]</sup> An example of the Hall effect data is presented in **Figure 3a** (the top panel), where sets of points show the temperature dependencies of the free electron concentration for two samples doped at different technological regimes. For both samples, initial FZ *p*-type silicon slightly doped with boron was used. The concentration of electrically active deep donors in a sample can be determined by the fitting of a calculated curve  $n(T)$  to the set of experimental points. A dependence  $n(T)$  can be deduced from the numerical solving of the charge-balance equation for a semiconductor, which in the considered case may be written as

$$n + N_B^- = p + N_{\text{Mg}}^{+/++} + N_X^+ \quad (3)$$

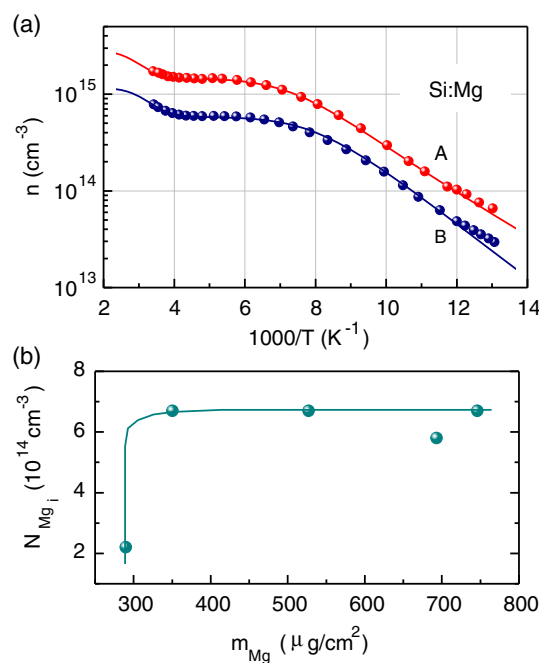


**Figure 3.** a) Typical temperature dependencies of the density of free electrons in Si:Mg samples prepared by the doping *p*-Si with a low boron content. Experimental points marked by (A) refer to a sample obtained by doping silicon with an initial resistivity of  $\rho = 3100 \Omega \text{ cm}$  for 1 h at  $T = 1200^\circ \text{C}$ . Data (B) correspond to a sample doped at  $T = 1100^\circ \text{C}$  for 2.5 h, where an initial *p*-Si with  $\rho \approx 450 \Omega \text{ cm}$  was used. Solid curves are temperature-dependent solutions to the charge balance Equation (3), which best describe the sets of the Hall effect data points. b) The concentration of interstitial magnesium in samples doped at different specific masses of magnesium  $m_{\text{Mg}}$  deposited on a wafer surface. Initial crystals were of *p*-type with a resistivity of  $450 \Omega \text{ cm}$ . The duration of the diffusion was 2.5 h at  $1100^\circ \text{C}$ .

where  $p$  is the concentration of free holes;  $N_{\text{B}}^-$  is the concentration of ionized shallow boron acceptors; and  $N_{\text{Mg}}^{+/++}$ , and  $N_{\text{X}}^+$  are singly/doubly ionized magnesium donor centers and other single-electron donors X, respectively.

When using the charge-balance equation in the above form, one proposes that over the whole temperature range, negatively charged species in the semiconductor volume are free electrons and charged shallow acceptors (the left part of the equation), while the positive charge is formed by free holes, as well as ionized magnesium centers and possibly other donors that may be in the ionized state. At a temperature in the range of 78–300 K, shallow acceptors are almost completely ionized; therefore, the value  $N_{\text{B}}^-$  in Equation (3) can be taken to be equal to the acceptor concentration defined by the resistivity of the initial silicon at room temperature. Depending on the position of the Fermi level in the crystal, an interstitial magnesium atom can be in neutral  $\text{Mg}^0$ , singly ionized  $\text{Mg}^+$ , and totally ionized state  $\text{Mg}^{++}$ .

Thus, the statistics of thermal equilibrium of a crystal containing a doubly charged donor differs from that corresponding to doping with two single-electron donors with different ionization energies. The corresponding problem for the case of doping a semiconductor with a multiply charged center has been theoretically treated in refs. [52,53]. On the basis of these works, the procedure for finding temperature-dependent solutions of the charge-balance equation for silicon doped with a deep double magnesium donor is considered in detail.<sup>[51]</sup> According to the optical absorption spectroscopy, the electron binding energies for  $\text{Mg}_i^0$  and  $\text{Mg}_i^+$  are 0.107 and 0.256 eV, respectively,<sup>[8,9]</sup> Using these values as trial parameters helps to determine the concentration of magnesium donors from the Hall effect data when fitting solutions  $n(T)$  of the charge-balance Equation (3) to experimental data. A proper fitting can be achieved by varying the concentrations of donors  $N_{\text{Mg}}$  and  $N_{\text{X}}$ , and when necessary, also slightly adjusting the ionization energies of centers. Solid lines in the graph of Figure 3a show the results of such fitting for two Si:Mg samples. The obtained partial concentrations of different centers in the samples are given in Table 1.

It can be seen that electron binding energies of double Mg donors, determined through the Hall method, fit well to those obtained by optical spectroscopy. The above example of applying the Hall method also shows that in addition to magnesium double donors, Si:Mg samples may contain relatively shallow centers with ionization energies of  $\approx 0.06$ – $0.08$  eV and concentrations of  $N_{\text{X}} = (4\text{--}9) \times 10^{13} \text{ cm}^{-3}$ . However, the Hall effect data in the used temperature range do not provide the accuracy required for the determination of parameters of such shallow centers, thus preventing their selective identification. The low-temperature

optical spectroscopy in the IR region makes it possible to measure the ionization energies of shallow donors with high relative accuracy, while the absolute accuracy is determined by the choice of the excited state to be matched to the theoretically obtained binding energy.<sup>[49]</sup> In a large number of cases, this enables a conclusion to be made about their nature, see Sections 4.4.1 and 4.4.4.

Applying the Hall effect measurements helps to optimize the technology of doping silicon with Mg. In particular, experiments have shown that to obtain samples of required dimensions with the uniform lateral distribution of interstitial magnesium, one has to use rather thick magnesium films evaporated on an initial wafer before diffusion. Figure 3b shows the concentration of  $\text{Mg}_i^0$  in samples found with the Hall technique, which is observed at applying different specific masses  $m_{\text{Mg}}$  of the deposited magnesium. (The  $m_{\text{Mg}}$  value refers to the sum of masses of the metal deposited on both sides of a wafer, while they are approximately equally covered with the metal.) The data show that the concentration of  $N_{\text{Mgi}}$  is practically independent of the  $m_{\text{Mg}}$  value at  $m_{\text{Mg}} > 350 \mu\text{g cm}^{-2}$  and is about  $\approx 7 \times 10^{14} \text{ cm}^{-3}$  for the given technology regime. One can see that decreasing  $m_{\text{Mg}}$  below this value leads to a sharp drop in the  $N_{\text{Mg}}$  concentration. We also note that strong inhomogeneities in the resistivity are observed in doped samples prepared at a small amount of the deposited magnesium.

To conclude this section: combining the temperature-dependent Hall effect measurements while simulating the effect of temperature on statistics of  $n$ -Si in the presence of double donors is a powerful instrument for the quantitative analysis of electrically active magnesium content in Si:Mg. As shown in refs. [51,54]—see Section 4.2—this enables the calibration of the absorption spectra of samples to a Mg concentration, which in turn enables the determination of the parameters of interaction of photons with the magnesium double donors.

### 3.4. Decomposition of a Solid Solution of Electrically Active Magnesium

The decrease in the concentration of electrically active magnesium as a result of heat treatment of Si:Mg was noted in one of the early studies in this area.<sup>[25]</sup> The thermal stability of a solid solution of interstitial magnesium in silicon was quantitatively investigated in ref. [55]. Si:Mg samples obtained by doping a high-purity FZ Si (resistivity  $\approx 8 \times 10^3 \Omega \text{ cm}$ , while oxygen and carbon concentrations did not exceed  $10^{15} \text{ cm}^{-3}$ ) with the sandwich method were used in the experiments. After doping (measured concentration of  $\text{Mg}^0$  donors was  $N_{\text{Mgi}}(300 \text{ K})$ ), samples were isothermally annealed in the temperature range 400–620 °C for various times. The annealing led to a decrease

**Table 1.** Examples of data for Si:Mg samples, as obtained from the temperature-dependent hall effect measurements (TH) and the low-temperature IR absorption spectroscopy. Samples were prepared using initial FZ Si crystals with different concentrations of compensating acceptors  $N_{\text{B}}$ , see Figure 3a.  $E_1$  and  $E_2$  are first and second ionization energies (that is, binding energies of electrons) for interstitial magnesium atoms in a different charge state.  $N_{\text{Mg}}$  and  $N_{\text{X}}$  are concentrations of interstitial magnesium and donors with lower ionization energies  $E_{\text{X}}$ , respectively.

Sample #		$E_1$ [eV]	$E_2$ [eV]	$E_{\text{X}}$ [eV]	$N_{\text{Mg}}$ [ $\text{cm}^{-3}$ ]	$N_{\text{X}}$ [ $\text{cm}^{-3}$ ]	$N_{\text{B}}$ [ $\text{cm}^{-3}$ ]
1–(99-2)	TH	0.105	0.256	0.08	$1.37 \times 10^{15}$	$9.0 \times 10^{13}$	$4.0 \times 10^{12}$
	IR	0.1075	0.2567	0.034–0.125			
2–(106-1)	TH	0.105	0.256	0.06	$5.8 \times 10^{14}$	$3.6 \times 10^{13}$	$2.8 \times 10^{13}$
	IR	0.1075	0.2567	0.047–0.125			

in conductivity, which indicated a decomposition of the solid solution of electrically active interstitial magnesium donors. The decrease of  $N_{\text{Mgi}}$  in some annealed samples was also directly observed by investigating optical absorption spectra at low temperature. The characteristic decomposition time of interstitial magnesium, as determined by measuring the samples' conductivity, decreased with an increase in the annealing temperature, see **Figure 4**. The estimated activation energy of the process is  $E_a = 1.6$  eV, which is close to the activation energy of diffusion of interstitial magnesium  $\approx 1.83$  eV, see Section 3.2. The data obtained in ref. [55] showed in particular that heat treatment could be used to controllably reduce the concentration of electrically active magnesium in Si:Mg samples.

A possible reason for the relatively low thermal stability of interstitial magnesium donors in silicon was discussed in a theoretical study.<sup>[56]</sup> The authors associated the phenomenon with the increased stability of silicide  $\text{Mg}_2\text{Si}$  centers as compared to  $\text{Mgi}$ . It is the high mobility of  $\text{Mgi}$  on interstitial sites that favors the formation of more stable Mg-related defect clusters during cooling of the sample to room temperature.

### 3.5. DLTS Characterization of Localized States in the Energy Gap of Si:Mg

Deep-level transient spectroscopy (DLTS) is known to be an efficient method for investigating deep localized states in semiconductors, e.g.<sup>[57]</sup> Until recently, there have been only a few publications on studies of Si:Mg that employ this technique.<sup>[21,58,59]</sup> In ref. [58], the investigated samples were prepared from silicon having different resistivity values by impurity diffusion from a magnesium film deposited on a semiconductor surface. The diffusion was performed in quartz ampoules at a temperature of 900–1200 °C for 15–90 min. After the process, an ampoule was cooled in air without special quenching. The authors

observed four discrete levels in the bandgap, for which energies were  $E_C - 0.18$ ,  $E_C - 0.25$ ,  $E_C - 0.38$ , and  $E_C - 0.4$  eV if counted from the conduction band edge. In the authors' opinion, they belonged to different magnesium-related centers and were not associated with multiply charged centers.

In ref. [21], samples doped with magnesium at a temperature of 1100–1200 °C for 1–5 h were investigated. Diffusion was performed from the magnesium vapor in sealed quartz ampoules. After the doping, the ampoules were quenched in mineral oil. From an analysis of obtained data, it was concluded that the sample doped at 1100 °C for 1 h contains amphoteric centers,  $\text{Mg(a)}$ , which are specified by levels at  $E_C - 115$  meV for the transition  $\text{Mg(a)}^{-/0}$  (an acceptor state) and by a donor state  $\text{Mg(a)}^{-/+}$  at  $E_C - 400$  meV. In the samples doped at 1200 °C, there were identified double donors,  $\text{Mg(d)}$ , which levels are at  $E_C - 107$  meV for  $\text{Mg(d)}^{0/+}$  transition, and at  $E_C - 310$  meV for  $\text{Mg(d)}^{+/2+}$  transition. Additionally, a  $\text{Mg(x)}^{0/+}$  donor state with an energy of  $E_C - 229$  meV was also detected in samples doped at 1200 °C.

DLTS spectra of  $n^+p$  structures prepared from commercial silicon diodes were investigated in ref. [59]. Magnesium was deposited on the front and back sides of a diode structure either by evaporation in vacuum or by ion implantation. To prevent the escape of magnesium during the diffusion process, a  $\text{SiO}_2$  layer was deposited on the surfaces of a diode. Doping was carried out in sealed quartz ampoules at a temperature of 950–1100 °C and for a duration of 1–4 h. At the end of the diffusion, the ampoules were quenched in a gas stream or in water. Several impurity levels in the lower half of the silicon bandgap were observed in the samples. In accordance with the obtained results, one of the levels—with an energy of  $E_v + 0.34$  eV—was the dominant center in most samples. The authors proposed that this level belonged to acceptor states caused by Mg atoms occupying substitutional positions in the lattice.

In a recent work,<sup>[60]</sup> the DLTS technique was applied to investigate samples obtained by doping with magnesium of  $n$ -Si with a resistivity of 0.5  $\Omega$  cm. Schottky diodes for DLTS measurements were prepared from the Si:Mg samples by the thermal evaporation of gold in vacuum. To provide a better temperature resolution of the DLTS signal, a variant of the method—a so-called Laplace-DLTS,<sup>[61]</sup>—was applied in the experiments. The results are shown in **Figure 5**, which contains DLTS spectra observed for the sample, both in the volume and near the surface. In both spectra, three peaks marked as  $E1$ ,  $E2$ , and  $E3$ , are observed.

When processing the experimental data, the ionization energies of observed donors have been evaluated, which are 252 meV for level  $E2$  and 215 meV and 112 meV for levels  $E3$  and  $E1$ , respectively.

While DLTS does not provide precise energies of localized states in the bandgap of a semiconductor, the above values of  $E1$ ,  $E2$ , and  $E3$  correspond to the values derived from optical spectroscopy: the ionization energies of neutral  $\text{Mgi}^0$  and singly ionized  $\text{Mgi}^+$  interstitial magnesium are 107.5 and 256 meV, respectively, while an “optical” energy of 215 meV is observed for singly ionized center  $\text{Mg}^*$ ,<sup>[62–65]</sup> (see below Sections 3.6 and 4.4.2).

Concentrations of levels  $E1$  and  $E2$  as determined from the DLTS in ref. [60] were close to the concentration of interstitial magnesium defined through the Hall effect measurements made on a control sample, which was doped under the same conditions. To ensure a high accuracy of data from the Hall effect

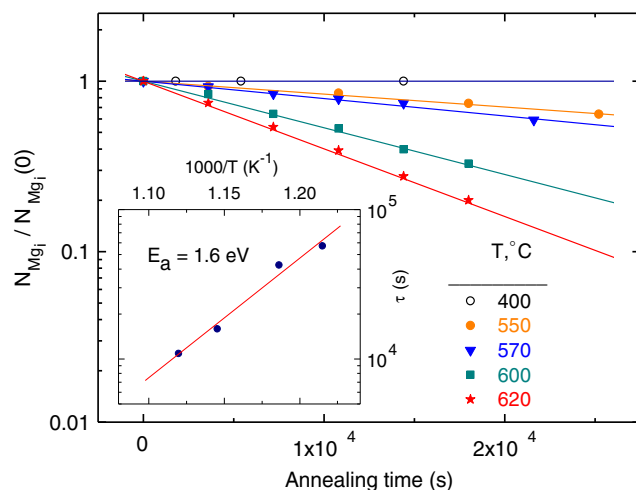


**Figure 4.** Effect of thermal annealing of doped Si:Mg samples on the concentration of interstitial magnesium at room temperature.<sup>[55]</sup> The concentrations of  $\text{Mgi}$  after annealing are normalized to its values before annealing. The inset shows the temperature dependence of the characteristic decomposition time of the  $\text{Mgi}$  solid solution. Adapted with permission.<sup>[55]</sup> Copyright 2019, Pleiades Publishing, Ltd.



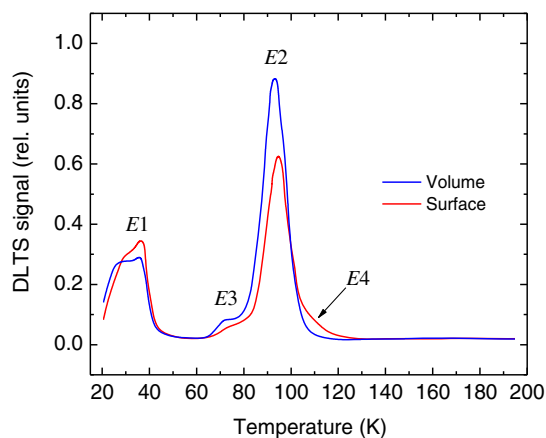


**Figure 5.** DLTS spectra for a Si:Mg sample prepared by doping a FZ *n*-Si with a resistivity of  $\rho = 0.5 \, \Omega \, \text{cm}$  at  $T = 1100 \, ^\circ\text{C}$ ,  $t = 2.5 \, \text{h}$ . The shown spectra are recorded for the sample volume and close to its surface. Adapted with permission.<sup>[60]</sup> Copyright 2019, Pleiades Publishing, Ltd.

measurements, a p-type silicon with a low boron content was used to dope the control sample.

As follows from the DLTS study, the concentration of the E3 level was  $\approx 10\%$  of the concentration of interstitial magnesium. Note also that the weak signal E4 in the DLTS spectra in Figure 5 was found only in the near-surface region. As proposed in ref. [60], the observed feature in the spectra may be due to a complex of magnesium with the hydrogen that could dope a subsurface region of the sample in the course of its chemical treatment prior to preparing the Schottky barrier. It should be noted that no DLTS signal in the spectra was observed at temperatures above  $\approx 120 \, \text{K}$ , which indicated the absence of the deeper donor states in the upper half of the bandgap of silicon (at least with a concentration exceeding  $\approx 5 \times 10^{12} \, \text{cm}^{-3}$ ) when compared with those discussed above.

It was also attempted to detect Mg-related deep acceptors in the lower half of the bandgap of silicon, while applying the DLTS of *p*-Si:Mg<sup>[66]</sup>; this trial was unsuccessful. Therefore, the existence of acceptor levels caused by substitutional magnesium atoms—as suggested in ref. [59]—was not supported by this experiment. However, data of ref. [59] may have been influenced by a contamination of samples by some other impurity forming deep centers.

In conclusion, the DLTS study appears to be complementary to the absorption spectroscopy with respect to the determination of binding energies and can prove the Hall measurements when determining the partial concentrations of different Mg donors in different charge states. A number of localized states in Si:Mg observed in DLTS spectra in some earlier publications without proof by optical absorption spectroscopy may be due either to the contamination of samples at their preparation or to an insufficient purity of initial silicon or magnesium. These circumstances may lead to the formation of complexes of Mg with unidentified impurities.

### 3.6. Absorption Optical Spectroscopy of Doped Samples

Electrically active centers in doped crystals can be characterized by low-temperature IR spectroscopy, e.g.<sup>[67]</sup> Such centers exhibit

atomic-like absorption lines that represent intracenter transitions from the ground to excited states of individual centers, and by this, may unambiguously identify their chemical composition. The intensities of unsaturated absorption transitions are related to the population of states. Thus, if appropriate calibration coefficients are used, the absorption spectroscopy data can provide information on the impurity concentration.

An overview of typical absorption spectra of Si:Mg samples measured in different spectral bands is shown in Figure 6. The data show absorption lines that belong to a number of Mg-related centers and centers that are not related to magnesium. Such data can give information on details of electronic states of optically active centers that are due to the presence of magnesium in crystals; for details, see Section 4.

With respect to problems of technology, the optical absorption spectroscopy at a low temperature has proven the presence of certain amounts of lithium in some *n*-Si:Mg samples prepared by the sandwich doping. When an initial silicon contains a significant concentration of dissolved oxygen, Li–O complexes can also be observed in samples doped with Mg.<sup>[68]</sup> Examples of such data are shown in Figure 6. The centers with the ionization energy of 32.81 meV refer to interstitial Li atoms, while donors with a slightly higher ionization energy of 39.41 meV correspond to Li–O complexes,<sup>[41,69]</sup> (note that a similar ratio of ionization energies is observed for interstitial Mg atoms and Mg–O complexes, see Section 4.4.4).

The appearance of lithium-related donors in the samples doped with magnesium of a purity up to 99.999% indicates that lithium is one of the impurities in the metal supplied by different companies and is introduced into samples during diffusion. To verify this assumption, experiments were carried out, where all procedures for preparing samples and their heat treatment were the same as in a standard doping routine, excluding the use of magnesium. The result was that such reference samples did not show lithium lines in the absorption spectra. Apparently, the presence of lithium in doped (Si:Mg) samples is associated

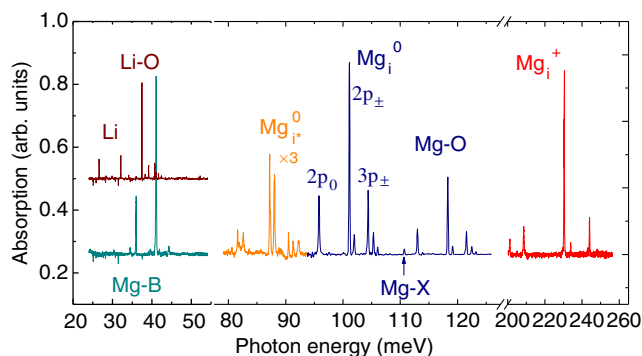


**Figure 6.** An overview of typical far- to mid-IR absorption spectra of Si:Mg samples. Shown are spectral bands that correspond to two charge states of the interstitial atomic Mg, to the neutral state of the center Mg\*, as well as to lithium- and boron-related donor centers. The Mg–X spectral line refers to an Mg-related complex of unknown origin. Raw data are obtained at samples temperature  $T = 10 \, \text{K}$ . To show characteristic features in spectra, the background signal, which varies slowly with the energy of photons, is subtracted when processing the data. Section 4 presents details about most of the spectra shown in figure.

with the problem of refining magnesium during the course of its production. Note that the absorption lines of lithium in the Si:Mg spectra are not always observed. A possible reason is that lithium can be trapped by defects on a sample surface during the high-temperature doping. Such gettering can be effective under appropriate conditions at samples' boundaries. In summary, it should be noted that the MIR spectra of samples unintentionally enriched with the lithium dopant reveal additional Mg-related complexes.<sup>[68]</sup>

Summarizing the above part of the review, we highlight that the use of the sandwich doping method provides high-quality bulk-doped Si:Mg samples. This enables a thorough study of the electrical and optical properties of the material, as well as investigating the effect of post-diffusion technological procedures on its parameters. The introduction of Mg into silicon initially doped with various impurities makes it possible to study its interaction with such impurities: magnesium can form complexes either with electrically inactive impurities or with elements whose atoms themselves create localized electronic states in the band gap. The complexes possess energy spectra that are different from those observed in the absence of the interaction of magnesium with such elements. Some examples illustrating these provisions are given in Section 4.4. Si:Mg co-doped with other optically active impurities can be used, for example, when designing photodetectors with an extended spectral band.

## 4. Optically Active Mg Centers and Mg-Related Complexes

Infrared spectroscopy enables us to simultaneously study both optically active (here: electrically active = optically active) isolated atomic  $Mg_i$  centers in different charge states and Mg-related complexes (Mg bound to other impurity atom/atoms). The presence of accompanying elements, which are either unavoidable at low concentrations in nominally pure Si crystals used at a preparation of Si:Mg samples or which are intentionally introduced into a silicon wafer before its doping with magnesium, can be proven both in an original silicon and after the doping procedure. Because some electrically neutral defects, such as interstitial oxygen, have IR active local vibration modes, their concentration, and its evolution in a crystal, as well as pairing with Mg, can also be tracked by repeated measurements over the course of a long-time sample storage at room temperature. Besides the activation energy, the complete energy spectrum of a center can be derived, including excited states of the same parity as the ground state, when they can be either thermally populated or can be seen in photoelectric spectroscopy experiments.

Along with the study of absorption spectra, useful information on localized states can be obtained by investigating the photoelectrical response of a sample to light quanta, for which energies are both lower and higher, when compared to the energy gap of Si. The first method is based on the population of excited states due to light absorption at intracenter transitions, while the interaction of the populated states with phonons gives rise to free carriers, and thus a sample photoconductivity. Thus, by exciting a sample with radiation of a variable wavelength, it is possible to investigate spectra of localized states in crystal, see one of the pioneer studies,<sup>[70]</sup> and review article.<sup>[71]</sup> Such photoelectric spectroscopy

was applied for Si:Mg samples in ref. [49]. In principle, by investigating the temperature dependence of photoelectric spectra, together with the use of an appropriate theoretical model, it is possible to obtain information on the dynamics of intracenter electronic relaxation.

Here, we review the main achievements of studying magnesium-related donors in silicon using IR spectroscopy.

### 4.1. Interstitial Magnesium Atom as a Helium-Like Donor

Detailed information on the energy structure of  $Mg_i$  is important when designing photonic devices based on Si:Mg. In particular, the donor energy spectrum determines the interaction of excited states with the phonon subsystem of the crystal, and thus parameters of nonequilibrium electronic distributions being created.<sup>[72,73]</sup>

While a group-V donor in silicon presents an analog of the hydrogen atom embedded into the solid matrix, double donors in the neutral states—chalcogens S, Se, and Te (and interstitial Mg)—may be regarded as helium-like centers. The present knowledge on the electronic structure of a magnesium atomic donor in the neutral ( $Mg_i^0$ ) and singly ionized ( $Mg_i^+$ ) states, as well as the  $Mg^*$  complex, is shown in Figure 7.

The excitation spectra of  $Mg_i^0$  are in many features similar to the spectra of shallow one-electron donors of the group V, which is due to the similar structure of the odd-parity excited states (*p*-, *f*-type) for single- and double-electron donors. An important difference is the existence of ortho-excited states in the spectrum of a He-like donor. The ortho-states (spin-triplet  $n^3$  state' stair) appear to be almost a replica of the spectrum of excited para-states (spin-singlet  $n^1$  state' stair). Their binding energies appear to be downshifted to the analogs in the para-spectrum, while this shift vanishes at high excited states. This is why many approaches use a modified hydrogen-like model for the model description of a helium-like center. For instance, one can consider the interaction between two electrons at the external shell and nucleus as the H-like, reduced owing to the partial screening of the nucleus potential by the "inner" electron, while the "outer" electron moves in the potential of a partially screened atomic nucleus. Wave functions of excited para- and ortho-states can be separately constructed using also the assumption of different orbital radii for the inner and outer electrons. Then, the inner electron is assumed to be unaffected by interactions with the outer electron and virtually moves in the Coulomb potential of the  $2+$  charged ion.<sup>[51]</sup> Under this assumption, well-developed effective mass theory (EMT) may be applied for the calculation of the energy spectra and also dipole moments of intracenter transitions,<sup>[51]</sup> resulting in a modified Rydberg-like para- and ortho-series of energy levels below the bottom of the conduction band.

In a more sophisticated approach to the problem, one has to take into account the complex structure of the conduction band of silicon, which consists of six equivalent valleys laying along the [001] axes in the reciprocal space. As a result, the localized donor states are degenerated by a factor of sixfold. Owing to the anisotropy of the electron effective mass in the valleys, the degeneration of donor states is lifted and appears to be spectroscopically resolved for the states with the largest chemical shift. The corresponding splitting of the states (which is referred to as

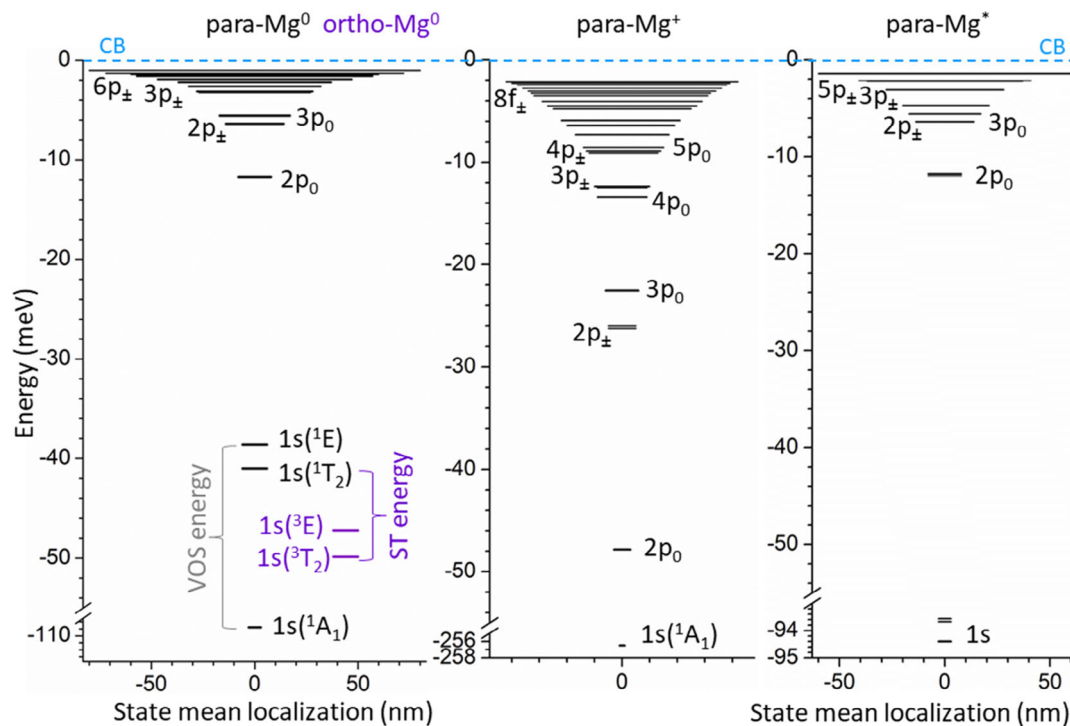


**Figure 7.** Energy diagram of bound electronic states of double magnesium donors in silicon as derived from optical spectroscopy. Left and center represent data for  $Mg_i$  in the neutral and singly ionized states, respectively. Right represents the scheme for an  $Mg^*$  complex in the neutral state. VOS—valley-orbit splitting, ST—exchange (spin-triplet) splitting energy. For detailed explanations, see the text. Data of studies<sup>[9,33,65,72,83,84,88]</sup> were used to prepare the diagrams.

valley-orbit splitting, VOS) occurs for the states that have a significant electron density at an impurity center site. Spherically symmetric  $s$ -states split into the  $A_1$ -state (not degenerate), the  $E$ -state (which is doubly degenerate), and the  $T_2$ -state (threefold degenerate).<sup>[74,75]</sup> The labels  $A_1$ ,  $E$ , and  $T_2$  refer to irreducible representations of the point group  $T_d$ , which is the point group of a substitutional or interstitial site of the silicon lattice. In the frame of this model, the spin of electrons is not taken into consideration.

The wave functions of the  $A_1$  ( $s$ )-states are symmetric, have large amplitudes at the center of a donor site, and as a result, are most sensitive to the true potential of the impurity atom, see e.g.,<sup>[76]</sup> The strongest valley-orbit splitting due to this effect—in the EMT it is called the central cell correction (CCC)—occurs for the deepest ( $1s$ ) state, while for higher  $ns$  and  $p$ ,  $d$ ,  $f$ ,... levels, it is negligible. Note that owing to the CCC, for most donors, the binding energy of the ground  $1s(A_1)$  state can differ significantly from the theoretical value obtained in the EMT.

Optical transitions from the ground  $1s(A_1)$  to  $p$ -,  $f$ -states are both dipole and symmetry allowed and are observed in absorption spectra of all shallow donors in silicon at low temperatures. Transitions from the ground to split-off states  $1s(A_1) \rightarrow 1s(T_2)$  are dipole forbidden but symmetry allowed, while transitions  $1s(A_1) \rightarrow 1s(E)$  are forbidden both in the dipole approximation and for symmetry reasons, i.e., they occur to be inactive in the IR absorption, but are Raman-active. It should be noted that transitions between split  $1s$  states are forbidden in the EMT model. While no optical transitions between  $1s$  states have been observed in silicon for shallow H-like donors with ionization energies in

the range of 43–54 meV, for deep He-like donors (S, Se, Te) whose ionization energies are between 200 and 610 meV, transitions  $1s(A_1) \rightarrow 1s(¹T_2)$  in absorption spectra at low temperatures have been detected.<sup>[77]</sup> As noted in ref. [78], this is because of the effect of states mixing, which increases with an increasing binding energy of the ground state. The effect is outside of the EMT model. Owing to the asymmetric component of the spin-triplet states, optical transitions from a singlet (para-state) ground state are not forbidden by a symmetry consideration. Such para-ortho transitions,  $1s(A_1) \rightarrow 1s(³T_2)$  were observed for Se and Te helium-like donors in Si, where the para-para transitions into the VOS state  $1s(A_1) \rightarrow 1s(¹T_2)$  are also presented in the spectra.<sup>[79]</sup>

However, for the Mg donor, such  $1s \rightarrow 1s$  transitions were not observed in low-temperature absorption spectra, while only the lowest valley-orbit-split triplet states have been determined for a neutral  $Mg^0$  center, as shown in Figure 7. However, such “dark” valley-orbit split states can be detected in experiments that combine the thermal population of these levels and studies of the optical transitions from them to the conduction band.<sup>[80]</sup>

#### 4.1.1. Details of Energy Spectrum of $Mg_i^0$ Defined by Valley–Orbit and Exchange Interactions

In addition to the valley-orbit interaction, the helium-like impurity undergoes the exchange interaction of two electrons that splits the VOS states into spin-singlet ( $¹T_2$ ) and deeper spin-triplet ( $³T_2$ ) terms.<sup>[81,82]</sup> The strength of the exchange splitting is characterized by the parameter  $\Delta_{ST}$  (Figure 7).

The position of the deepest VOS state of  $\text{Mg}_i^0$  was first estimated in ref. [9] by scaling piezo-spectroscopic data, which gave a value of  $56.24 \pm 3$  meV. The experimental data for the binding energies of the deepest VOS states for the  $\text{Mg}_i^0$  center were first obtained in ref. [83]. A sample with a relatively high magnesium concentration exceeding  $10^{15} \text{ cm}^{-3}$  was used in the experiments. Binding energies of  $1s(E)$  and  $1s(T_2)$  states were defined by recording absorption spectra of the sample at thermally populating VOS states with electrons at an increase in temperature, which made it possible to observe dipole-allowed transitions from the  $1s(E)$  and  $1s(T_2)$  states into  $2p_{\pm}$  levels, i.e., those with the largest oscillator strengths. Considering that the binding energy of the  $2p_{\pm}$  level is 6.38 meV,<sup>[9]</sup> the energies of the  $1s(E)$  and  $1s(T_2)$  states of the  $\text{Mg}_i^0$  center were determined by adding this value to the energies of the observed transitions, see Figure 7. As a result, the electron binding energies for the  $1s(E)$  and  $1s(T_2)$  states were evaluated in ref. [83] as  $47.4 \pm 0.1$  and  $49.9 \pm 0.1$  meV, respectively. This finding was then confirmed in studies.<sup>[72,84]</sup> According to ref. [84], the binding energies for the  $1s(^1E)$  and  $1s(^1T_2)$  states are 47.20 and 49.86 meV, respectively. An analysis of the MIR absorption spectra of Si: Mg under an uniaxial stress together with the observation of the Fano-type intracenter resonances in the photocurrent spectra of Si:Mg was performed.<sup>[72]</sup> This enabled data to be obtained on the VOS states with lower binding energy and provided the identification and separation of the singlet (binding energies of  $1s(^3T_2)$  and  $1s(^3E)$  states, which were 41 and  $\approx 38.66$  meV, respectively) and triplet-VOS states (binding energies of  $1s(^3E)$  and  $1s(^3T_2)$  states are 47.5 and 49.9 meV, respectively) of the  $\text{Mg}_i^0$  center.

The binding energies of the split-off levels (39–50 meV) of the Mg ground state significantly exceed the corresponding values for other investigated donors in Si. For shallow substitutional group-V, as well as for interstitial group-I impurities, the  $1s(E)$  state has a binding energy in the range of 30.17–32.61 meV.<sup>[83]</sup> These values are relatively close to the binding energy in the frame of the EMT (which for the energy of  $1s$  state gives  $1s(A_1) = 1s(E) = 1s(T_2) = 31.26$  meV.<sup>[82]</sup>) For the substitutional group-VI deep double chalcogen donors, S, Se, and Te in Si (ionization energies  $\approx 0.2$ – $0.3$  eV), the binding energy for the  $1s(E)$  state are within 31.4–34.6 meV.<sup>[76,82]</sup> In contrast, the splitting between singlet and triplet VOS states ( $1s(E)$ – $1s(T_2) = 2.4$  meV) of a two-electron  $\text{Mg}_i^0$  center is within the range of those for the one-electron donors in Si, 0.316–4.118 meV,<sup>[82]</sup> as well as to those for the deepest double donor centers, sulfur and selenium, where it is about 3 meV.

It is instructive to compare parameters of  $\text{Mg}_i^0$  that are determined in refs. [7,83,84] with corresponding data for chalcogen double donors in neutral states, see Table 2, where binding energies of  $A_1$ ,  $T_2$ ,  $E$  states, and values of  $\Delta_{\text{ES}}$  for these impurity centers are given. The following trend is observed for chalcogens: The  $1s(T_2)$  binding energy is the largest for Te when compared to other chalcogens, while Te has the smallest electron binding energy. It should be noted that  $\text{Mg}_i^0$  also follows the trend: Having the smallest ionization energy among other double donors in the series, Mg exhibits the largest  $1s(T_2)$  binding energy. The two bottom rows in Table 2 present energy spacing between ground states and triplets  $1s(^1T_2)$  and  $1s(^3T_2)$ , respectively, which are split by the exchange interaction.

**Table 2.** Binding energies of valley orbit split states and exchange interaction energies for deep double donors in silicon.

State	S <sup>0</sup> [meV]	Se <sup>0</sup> [meV]	Te <sup>0</sup> [meV]	Mg <sup>0</sup> [meV]
$1s(A_1)$	318.3 <sup>a)</sup>	306.6 <sup>a)</sup>	198.8 <sup>a)</sup>	107.5 <sup>b)</sup>
$1s(^1T_2)$	34.6 <sup>a)</sup>	34.4 <sup>a)</sup>	39.1 <sup>a)</sup>	41.0 <sup>c)</sup>
$1s(^3T_2)$	–	40.62 <sup>b)</sup> , 40.45 <sup>d)</sup>	47.72 <sup>c)</sup>	49.9 <sup>f)</sup>
$1s(E)$	31.6 <sup>a)</sup>	31.2 <sup>a)</sup>	31.6 <sup>a)</sup>	47.4 <sup>f)</sup>
$\Delta_{\text{ST}}$	–	6.01 <sup>b)</sup>	7.56 <sup>c)</sup> , 8.12 <sup>b)</sup>	8.9 <sup>h)</sup>
$1s(A_1) \rightarrow 1s(^1T_2)$	283.7	272.2	159.7	66.5
$1s(A_1) \rightarrow 1s(^3T_2)$	–	266.2	151.08	57.6

<sup>a)</sup>Ref. [98]. <sup>b)</sup>Ref. [99]. <sup>c)</sup>Ref. [81]. <sup>d)</sup>Ref. [79]. <sup>e)</sup>Ref. [72]. <sup>f)</sup>Ref. [83].  
<sup>g)</sup>Ref. [8]. <sup>h)</sup>Defined from data in Refs. [72,83].

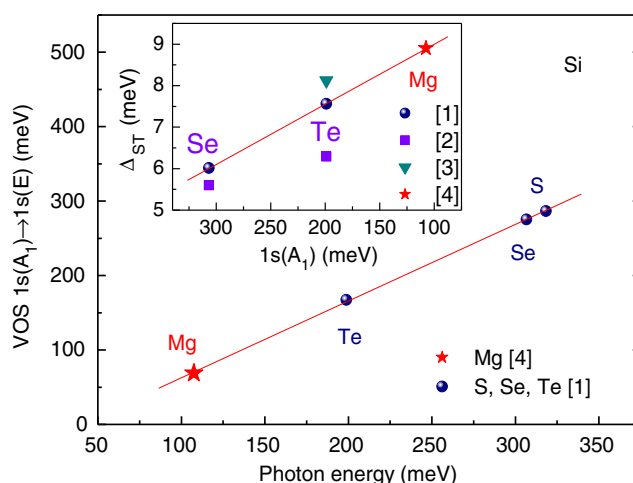


**Figure 8.** Main panel—energy spacing between the ground and the VOS-split  $1s(E)$  states as a function of the ionization energy  $E_i$  of atomic double donors in silicon.<sup>[72,83,98]</sup> The inset shows how the electron exchange interaction energy  $\Delta_{\text{ST}}$  for the  $1s(T_2)$  state depends on the  $E_i$  value of donors. The data are collected from: 1—Ref. [81]; 2—Ref. [79]; 3—Ref. [99]; 4—Refs. [72,83].

The discussed dependencies of parameters on the ionization energy for the set of double donors in Si are clearly seen in Figure 8. It is remarkable that the electron–electron interaction in two-electron deep donors in silicon becomes more pronounced at a decreased ionization energy.

## 4.2. Oscillator Strengths for Intracenter Transitions of Neutral $\text{Mg}_i$

Oscillator strengths of impurity absorption transitions give quantitative information that can be used for different applications: from the optical calibration of electrically active impurities to sophisticated optical studies that rely on relevant infrared intracenter transitions. To characterize the absorption of light at some spectral line, one can calculate the integral absorption  $A$  for a center



$$A = \int_{\text{line}} \alpha(\nu) d\nu \quad (4)$$

where  $\alpha(\nu)$  is the measured absorption coefficient ( $\text{cm}^{-1}$ ),  $\nu$  is the wave number ( $\text{cm}^{-1}$ ); integration is performed over the line curve.

The oscillator strength  $f$  of a transition can be obtained from the relation<sup>[85,86]</sup>

$$f = \frac{n\bar{m}}{2\pi^2\hbar e^2} \frac{1}{N} \int_{\text{line}} \alpha(\nu) d\nu = \frac{9.88 \times 10^{11}}{N} \int_{\text{line}} \alpha(\nu) d\nu \quad (5)$$

where  $n$  is the refractive index of silicon in the given spectral region,  $n = 3.38 \cdot (1 + 3.9 \times 10^{-5} T)$ ,  $\bar{m} = [(2m_t^{-1} + m_l^{-1})/3]^{-1}$  is the average electron mass, which is determined by the combination of the transverse  $m_t$  and longitudinal  $m_l$  effective masses of electron in the valley of the conduction band of silicon.  $c$ ,  $\hbar$ , and  $e$  are the speed of light, Planck's constant, and the electron charge, respectively. The dimensionality of the numerical factor is  $[\text{cm}^{-1}]$ .

Using the data of optical absorption spectroscopy and relationships (4,5), the integral absorption cross sections (and oscillator strengths  $f$ ) were found in ref. [54] for the lines  $\rightarrow 2p_0$  and  $\rightarrow 2p_{\pm}$  of neutral magnesium, which are  $A/N = 7.7 \times 10^{-15}$  and  $2.0 \times 10^{-14} \text{ cm}^2$  ( $f = 0.0076$  and  $0.0165$ ), respectively. In these estimates, the partial concentrations of  $\text{Mg}^0$  centers in samples were derived using the temperature-dependent Hall measurements (see Section 3.3). We note that calibrated optical characteristics permit the determination of the impurity concentration in a sample by optical spectroscopy. The derived calibration factors when using two absorption lines of  $\text{Mg}^0$  are as follows

$$N_{\text{Mg}^0}(\text{cm}^{-3}) = 1.61(05) \times 10^{14}(\text{cm}^{-1}) \times \alpha_{\rightarrow 2p_0}(\text{cm}^{-2}), \text{ and} \\ N_{\text{Mg}^0}(\text{cm}^{-3}) = 7.18(09) \times 10^{13}(\text{cm}^{-1}) \times \alpha_{\rightarrow 2p_{\pm}}(\text{cm}^{-2}) \quad (6)$$

where  $\alpha_{\rightarrow 2p_0/2p_{\pm}}$  is the integrated absorption of the intracenter transition into the corresponding excited state of an  $\text{Mg}^0$  donor.

In ref. [51], a systematic study that focused on finding parameters  $\alpha$  and  $f$  for the most well-known double donors in silicon—chalcogens (atomic S, Se and diatomic  $\text{S}_2$ ,  $\text{Se}_2$  centers), as well as the interstitial magnesium in the neutral state—was performed. These parameters were also estimated for a double center  $\text{Mg}^*$ . A large set of samples doped with different concentrations of impurities was used in experiments to improve the statistics. Moreover, not only were the strongest absorption lines of donors investigated (as in the work<sup>[54]</sup>) but also a number of higher excited states of the centers. The parameters of interaction of electromagnetic radiation with the states of deep donors were compared with the corresponding data known for hydrogen-like donor centers (see Figure 9), where oscillation strengths for intracenter transitions terminating in the  $2p_{\pm}$  and  $2p_0$  states for single- and two-electron donors are shown. Among the main results of the study<sup>[51,54]</sup> are experimental dependencies of the absorption cross section and oscillator strength on the ionization energy of deep donors. In accordance with the data obtained, a strong deviation of these parameters from the dependence that would be expected from the study of shallow donors in Si was observed.

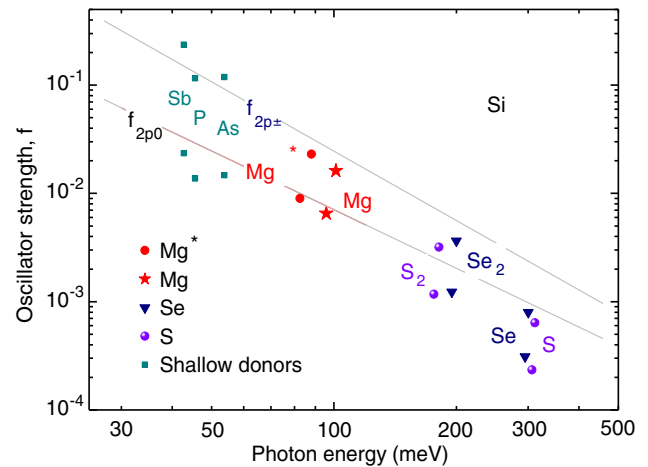


**Figure 9.** Oscillation strengths for  $\rightarrow 2p_{\pm}$  and  $\rightarrow 2p_0$  transitions for deep He-like and shallow H-like donors in silicon. The data are collected from refs. [51,54]. Original data for shallow donors are taken from refs. [67,85,86,100]. The solid lines approximate data for shallow donors<sup>[85]</sup> and extend to larger ionization energies.

### 4.3. Singly Ionized Magnesium Double Donor

Singly charged interstitial magnesium in silicon  $\text{Mg}_i^+$  (see the corresponding spectral band in Figure 6 and energy diagram in Figure 7) can be observed in samples, where Mg donors are partly compensated by acceptors or radiation-induced defects.<sup>[9,87]</sup> Compensated samples can be prepared by using initial silicon doped with the boron acceptor. A high content of  $\text{Mg}_i^+$  can be achieved for a specific range of acceptor concentration, which provides a partial compensation of the deep double Mg donor. When the acceptor concentration is too high –  $N_A > 2N_{\text{Mg}}$  – all magnesium centers are in the  $\text{Mg}_i^{++}$  states at a low temperature.

If one considers an  $\text{Mg}_i^0$  center being similar to the helium atom embedded into the crystal lattice,  $\text{Mg}_i^+$  can be regarded as an analog of the singly ionized helium, where one of its two 3s valence electrons is lost through the compensation by an acceptor. The effective charge  $Z$  of the center core is then  $2+$ . Thus, the spectrum of excited states of  $\text{Mg}_i^+$  should be similar to the spectrum of donors of group-V (and  $\text{Mg}^0$ ), except that the electron binding energies should be increased by a factor of  $\approx 4$  when compared to the states of an H-like donor. Excitation spectra of  $\text{Mg}_i^+$  in silicon have been previously studied in a number of works, e.g., see refs. [9,33,88]. The earlier results are summarized in detail in the review.<sup>[82]</sup>

A recent comparative study of the FZ (Si:B):Mg samples with an increased concentration of  $\text{Mg}_i^+$  centers and different isotopic contents of Si revealed new important results.<sup>[65]</sup> Samples prepared from Si with natural isotope content and isotopically enriched crystals ( $^{28}\text{Si}$  content was 99.995%) were used. The boron concentration in the initial crystals was  $2.2 \times 10^{15}$  and  $1.8 \times 10^{15} \text{ cm}^{-3}$ , respectively. The samples were doped with Mg at a temperature of 1250 °C for 7.5 h. Binding energies of excited states up to the  $8f_{\pm}$  level were determined for  $\text{Mg}_i^+$ . It is possible to observe higher quantum states in  $\text{Mg}_i^+$  because the energy spacing between the corresponding spectral lines for this center is four times larger when compared to  $\text{Mg}_i^0$ , as

previously mentioned. The data illustrate that the energy difference between the  $2p_0$  and  $2p_{\pm}$  states is 21.86 meV, while for  $\text{Mg}_i^0$ , the corresponding value is 5.32 meV. A distinctive feature of the excitation spectra of  $\text{Mg}_i^+$ , as noted by various authors (e.g.,<sup>[9]</sup>) is the fine splitting of the  $p_{\pm}$  states and corresponding intracenter transitions. The splitting is the largest for the  $2p_{\pm}$  level and decreases with an increase in the quantum number of a state. In accordance with the conception discussed in ref. [33], splitting of the  $2p_{\pm}$  states is of the same origin as the chemical shift of the  $\text{Mg}_i^+$  ground state compared with the EMT value. That is, it is caused by a central-cell perturbation (CCC), which is due to a deviation of the real short-range potential from the long-range screened EMT potential. A spectrally resolvable isotopic shift (10–30  $\mu\text{eV}$ ) has been obtained for the intracenter transition of an  $\text{Mg}_i^+$  center.<sup>[65]</sup>

#### 4.4. Mg-Related Complexes

Magnesium impurity in silicon occurs to be active in the form of different complexes, both with substitutional and interstitial impurities in silicon.

##### 4.4.1. Pairing of Mg with Substitutional Acceptors (Group-III Elements) with the Formation of Shallow Donors (Mg–A Complexes)

The observation of shallow donors with an ionization energy of 47.50 meV in absorption spectra of Si:Mg samples was reported from as early as 1973.<sup>[19]</sup> Because silicon used for the doping contained boron and oxygen, the authors assumed that these donors may be either Mg–O or Mg–B complexes.

In recent works,<sup>[65,89]</sup> Si:Mg samples obtained by doping *p*-Si with Group-III acceptors (A = B, Ga, Al, and In) have been investigated. It was found that magnesium forms electrically active donor complexes with these substitutional impurities (Mg–A complexes). **Figure 10a** shows absorption spectra of samples prepared from initial silicon doped with group-III acceptors in the course of silicon growth. The ionization energies of Mg–B,

Mg–Al, Mg–Ga, and Mg–In complexes were evaluated as 47.48, 60.24, 54.51, and 55.15 meV, respectively. It has also been established that the ionization energy of an Mg–A donor and the localization energy of the excitons on it obey the well-known Haynes rule,<sup>[90]</sup> see **Figure 10b**, which supports the above interpretation of the absorption spectroscopy data. We note that refs. [65,89] expand the range of ionization energies of singly charged donors in silicon, for which the Haynes's rule is observed.

Note that the above sequence of the ionization energies of shallow donors does not correlate with the tendency in a change in the binding energies of acceptors (A): For the corresponding impurities, this is as follows (Si:A): 45.63 (:B), 70.36 (:Al), 74.04 (:Ga), and 156.90 (:In) meV.

As in ref. [89], complexes of Mg with shallow acceptors are formed at a high temperature of samples processing owing to the attractive electrostatic interaction between an ionized Group-III acceptor in the  $-1$  charge state and a double donor  $\text{Mg}_i$  in the  $2+$  charge state. This gives the same net valence of a complex, as with the Group-V shallow donors.

##### 4.4.2. Deep Donors $\text{Mg}_i^0/\text{Mg}_i^+$

New donor states in Si:Mg with a lower ionization energy compared to a neutral  $\text{Mg}_i^0$  center were observed in studies<sup>[62,64]</sup> when investigating the absorption spectra of samples at a temperature close to that for liquid helium. A part of the spectrum of a sample containing such centers is shown in **Figure 6**. In the pioneer study,<sup>[62]</sup> the authors interpreted the complicated detailed absorption features in the spectra as belonging to two centers with energies that are close to their ground states. The ionization energies of these centers were evaluated as 93.57 and 94.36 meV.

However, in a recent investigation,<sup>[65]</sup> it was proven that the features in absorption spectra of Si:Mg discovered in ref. [62] correspond to one center, which is a single perturbed  $\text{Mg}_i$  species. (It was proposed to call it  $\text{Mg}_i^*$ .) Such a conclusion was based on the observation that a temperature increase in the range of

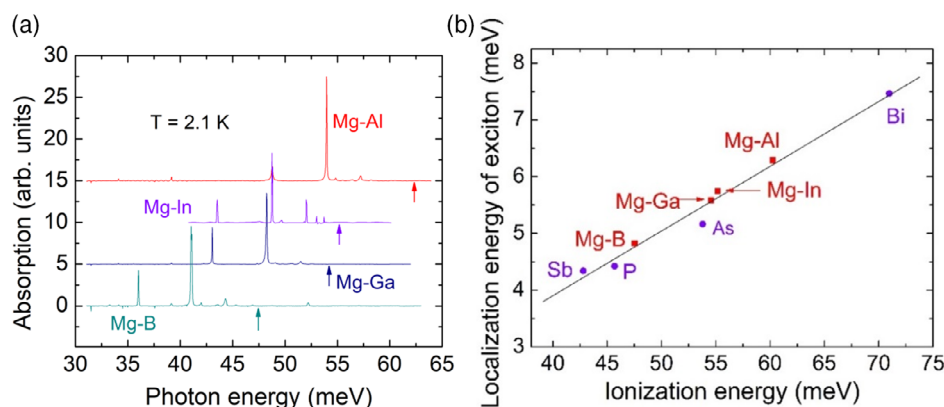


**Figure 10.** a) Excitation spectra of Si:Mg:A samples in the far IR that show the presence of Mg–A complexes. Arrows indicate the ionization energies of the complexes. b) The observed relationship between the ionization energy of shallow donors in Si and the energy of localization of excitons on the donors (the Haynes rule,<sup>[90]</sup>). Luminescent data for pairs Mg–Ga, Mg–In, and Mg–Al were obtained at  $T = 1.4$  K and for Mg–B at  $T = 4.2$  K. The data presented in the Figure are graphically adapted results obtained from refs. [65,89]. Adapted with permission.<sup>[65]</sup> Copyright 2018, American Physical Society. Adapted with permission.<sup>[89]</sup> Copyright 2019, American Physical Society.

2.1–10 K is accompanied by an expressed change in the relative intensities of intracenter  $\text{Mg}_{\text{is}}^*$  transitions. According to Ref. [65], the effect is due to a specific energy structure of the  $\text{Mg}_{\text{is}}^*$  center, exhibiting a fine VOS of its ground state. Being a double donor, in the neutral state, it has a series of levels that are located slightly (less than 1 meV) above the ground state (Figure 6). Therefore, a temperature increase above 2.1 K leads to the thermal population of these VOS states, which can be seen through the appearance of optical transitions from them to the higher excited odd-parity states. At some intermediate temperature, both series of lines (from the ground and VOS states) can be seen in infrared spectra. According to the results,<sup>[65]</sup> ionization energies of the neutral and singly charged  $\text{Mg}_{\text{is}}^*$  centers are 94.36 and 213.53 meV, respectively. These values were estimated by the summation of the transition energies from the ground state to the  $4p_{\pm}$  level, assuming that the binding energy of the  $4p_{\pm}$  level is equal to the theoretically calculated values, which are 2.187 and 8.75 meV for the neutral and ionized species, respectively.

The appearance of  $\text{Mg}_{\text{is}}^*$  centers in Si:Mg samples depends on the diffusion regime and a post-diffusion thermal annealing. A short-time annealing at 1200 °C with subsequent rapid quenching, which is performed by dropping the sample into alcohol, destroyed the  $\text{Mg}_{\text{is}}^*$  centers.<sup>[65]</sup> A similar effect was observed in rapidly cooled samples, where an ampoule with a sample was dropped into a mineral oil just after the diffusion doping.

We note that the manifestation of a very small chemical shift—between the ground and the VOS state(s)—in the energy spectrum of the  $\text{Mg}_{\text{is}}^0$  center is quite unusual for donors in silicon, and has not yet been supported by theoretical interpretation: single-electron donors in silicon exhibit VOS above 10 meV, while VOS above 70 meV are typical for two-electron centers.

Unlike the  $\text{Mg}_{\text{i}}^+$  center, for which the  $2p_{\pm}$  state is split into a doublet, the corresponding transition for  $\text{Mg}_{\text{is}}^+$  has a more complex structure. As shown in ref. [65], by decomposing the line profile into spectral components, it can be fitted by four mixed Gauss–Lorentz peaks. The observed reduction of the configuration symmetry of an  $\text{Mg}_{\text{is}}^*$  center to the  $C_v$  type from that specific for the interstitial Mg of the  $T_d$  symmetry may be due to the creation of a complex of the interstitial magnesium with some other impurity, or with a lattice defect.

With respect to the discussed “enigmatic” Mg-related center, it is appropriate to cite ref. [10], where silicon doped with magnesium was investigated using the electron paramagnetic resonance technique. An implementation of the method is provided by the fact that a singly ionized magnesium atom in the silicon lattice has an unpaired electron at the outer shell. In these experiments, the authors used compensated samples obtained by magnesium doping a FZ *p*-Si with a boron concentration of  $\approx 1 \times 10^{15} \text{ cm}^{-3}$ . It was found that at the thermal equilibrium at a low temperature—near the liquid helium value, magnesium ions  $\text{Mg}^+$  occupied the tetrahedral interstitial positions in the dark. Under illumination of the crystal by the near-IR light, magnesium paramagnetic centers  $\text{Mg}^+$  were converted to metastable states, which the authors called  $(\text{Mg}^+)^*$ . Such a state corresponded to the  $\text{Mg}^+$  ion displaced from the position of the  $T_d$  symmetry to the interstitial site located along the  $\langle 111 \rangle$  axis of the silicon unit cell, which may be the  $C_{3v}$  hexagonal position. When the illumination was turned off, the system slowly relaxed, that is, the centers returned into states with the initial symmetry.

This phenomenon appears to be related to a small energy barrier between two positions of an Mg atom in the interstitial position of the lattice. Such a “flexibility” of magnesium in silicon may be in favor of its pairing with either another Mg atom or an impurity atom.

If the pairing of magnesium atoms can give electrically active centers, there could be considered an analogy of this phenomenon with the effect of pairing of chalcogen atoms S, Se, and Te in silicon.<sup>[76]</sup> Similar to isolated atoms, chalcogen pairs are double donors, which are specified by lower ionization energies when compared to single atoms. An estimation of the  $\text{Mg}^*$  concentration in samples through the analyses of the strength of optical intracenter transitions gave the value reaching  $\approx 20\%$  of Mg<sub>i</sub> in moderately doped Si:Mg,<sup>[51]</sup> while estimates from the DLTS experiments of a few, lower doped, Si:Mg samples limited its relative concentration to a maximum of  $\approx 10\%$ .<sup>[60]</sup>

#### 4.4.3. Isoelectronic Mg–Mg Pairs

A conception of Mg pairs in silicon was advanced,<sup>[25]</sup> to interpret the observation of a large Mg concentration that did not exhibit electrical activity. It was proposed that magnesium can form electrically neutral isoelectronic pairs of atoms. Such a pair comprises substitutional  $\text{Mg}_{\text{s}}$  and interstitial  $\text{Mg}_{\text{i}}$  atoms, while similar to the well-known isoelectronic center of beryllium in silicon,<sup>[91]</sup> does not create a localized electronic state in the band gap. In ref. [34], it was proposed to interpret features in photoluminescence (PL) spectra of Si:Mg as a recombination of excitons localized at the isoelectronic magnesium pairs.

The effect of the PL of Si:Mg was recently reexamined.<sup>[46]</sup> Experiments were carried out using samples prepared from the highly enriched  $^{28}\text{Si}$  as an initial material, which enabled the resolution of the fine structure of defects and impurity centers in the PL spectra. It was found that the spectrum at  $T = 2.1 \text{ K}$  can be resolved in five lines, see Figure 11. Their relative intensities corresponded to random combinations of pairs of three stable naturally occurring Mg isotopes:  $^{24}\text{Mg}$ ,  $^{25}\text{Mg}$ , and  $^{26}\text{Mg}$ . The total masses of such centers range from 48 to 52 atomic units as dependent on combinations of isotopes, with  $^{24}\text{Mg}$ – $^{24}\text{Mg}$  comprising the largest fraction and  $^{26}\text{Mg}$ – $^{26}\text{Mg}$  the smallest. This observation unambiguously proved the existence of pairs of Mg atoms in Si:Mg. At the same time, it remains unclear whether there is a connection between the electrically active  $\text{Mg}_{\text{is}}^*$  centers discussed above in Section 4.4.2 and the Mg–Mg pairs found in ref. [46].

#### 4.4.4. Pairing of Mg with Interstitial Impurities

Magnesium is capable of interacting with other interstitial impurities in silicon, thus forming complexes with them. The most studied is the complex Mg–O. Its finding dates back to the publication,<sup>[33]</sup> where a donor with a higher ionization energy (124.69 meV) compared to  $\text{Mg}_{\text{i}}^0$  was observed in the photoexcitation spectra of Si:Mg. In ref. [92], this center was identified as a complex of magnesium with oxygen, see Figure 6. During the course of a further study, the effect of the accumulation of Mg–O centers in Si:Mg crystals during their long-time storage (months and years) at room temperature was established.

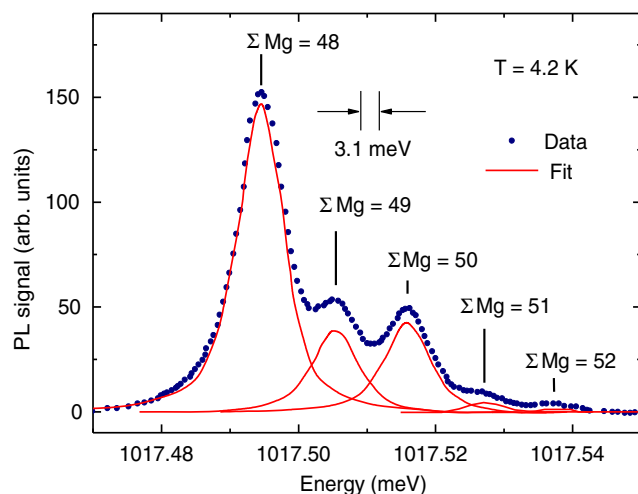


**Figure 11.** Luminescence spectrum of Si:Mg that shows the presence of magnesium pairs in a sample prepared from the isotope  $^{28}\text{Si}$ -enriched silicon. The spectrum is obtained at a resolution of 3.1  $\mu\text{eV}$ , while exciting the sample by a 1031 nm laser. The combination of three Mg isotopes gives five pairs with different masses, which are resolved in the luminescence spectrum. For further comments, see the text. The data presented in the figure are results obtained in ref. [46] and adapted with permission.<sup>[46]</sup> Copyright 2018, the American Physical Society.

This process was accompanied by a decrease in the concentration of interstitial magnesium.<sup>[93]</sup> Because the diffusion coefficient of oxygen in silicon is relatively low (for example, at  $T = 1000^\circ\text{C}$ , the  $D_{\text{ox}}$  value is  $\approx 10^{-10} \text{ cm}^2 \text{ s}^{-1}$ ,<sup>[94]</sup> it can be assumed that the accumulation of Mg–O complexes during the storage of a sample at room temperature has to proceed through the diffusion transport of magnesium in the lattice. One can estimate the magnesium diffusivity that is required for such a process at room temperature. For example, let us assume that the diffusion transfer of magnesium atoms during, say  $10^8 \text{ s}$  (approx. three years), should occur at the length of order  $\approx 10 \text{ \AA}$ . This is possible if the diffusion coefficient has a value of at least  $\approx 10^{-22} \text{ cm}^2 \text{ s}^{-1}$ . However, extrapolating the observed temperature dependence of the magnesium diffusion coefficient, expression (1) in Section 3.2, to room temperature, we obtain  $D_{\text{Mg}}(T = 300 \text{ K}) \approx 5 \times 10^{-31} \text{ cm}^2 \text{ s}^{-1}$ . Such a significant difference between both estimates indicates that the extrapolation of the high-temperature Mg diffusivity to a low-temperature is incorrect. Thus, the mechanism of interstitial magnesium transport, which determines the relatively fast kinetics of the formation of Mg–O complexes observed at room temperature, remains unclear.

Another example of pairing magnesium with an interstitial impurity is the apparent formation of Mg–Li complexes that exhibit properties of H-like shallow donors.<sup>[68]</sup> In that work, the influence of the strong magnetic field on spectra of different Mg-related donor centers in Si:Mg was investigated.

#### 4.5. Other Mg-Related Donors

A detailed analysis of the excitation spectra of Si:Mg shows that a number of other Mg-related donors with ionization energies ranging from  $\approx 40$  to  $\approx 130 \text{ meV}$  may be observed in Si:Mg

samples, see Tables 3 and 4 in ref. [95]. Because the origin of these donors has not been established up to the present, in the present review, we refer to them as Mg–X centers. They can be seen in the absorption spectra of samples prepared by doping of both conventional high-resistivity FZ Si and high-purity crystals.

The nomenclature and concentrations of these donors observed in a sample depends on the doping and cooling regimes of its preparation process. It has also been observed that some donors demonstrate a long-term evolution that is similar to that established for the Mg–O complex discussed in Section 4.4.4. An example of such an Mg–X center is presented by Figure 6, where its strongest absorption line is shown. In ref. [31], an accumulation of these Mg–X donors was demonstrated over the course of several months and years. When investigating the energy spectrum of the center, its ionization energy was evaluated as 119.3 meV.<sup>[95]</sup>

While the phenomenon of the generation of the multiplicity of donors in Si:Mg is quite complicated and requires a further study, some approaches to interpret the experimental findings are proposed in ref. [95]. Possible models are based on the results of investigations in which similar phenomena are observed for other impurities in silicon. It has been long established that the formation of so-called thermal donors (TDs) is related to the aggregation of oxygen dissolved in silicon, e.g.<sup>[76]</sup> By analogy with this mechanism of TD formation in oxygen-enriched silicon, we can assume that some Mg–X centers are electrically active clusters of magnesium atoms embedded in the crystal lattice: Their bonds with the nearest silicon atoms generate various configurations of clusters. The multiplicity of centers observed in IR-absorption appears to reflect different scenarios in the growth and evolution of electrically active Mg clusters in the course of doping, subsequent cooling, and further thermal treatment of the samples. We stress that such a scenario does not require the presence of other impurities in an Si crystal.

Note that other chalcogens—S, Se, and Te—are known to form multiplicities of donor centers in silicon. While occupying substitutional positions in the lattice, atoms of these elements can create clusters that consist of either the same chalcogen atoms or of a mixture of them. A number of such donor centers in silicon was found, and an important observation is made in that the binding energy of electrons to such a cluster decreases with an increase in the number of atoms in it, see the review article.<sup>[76]</sup> These experimental data are supported by the theoretical study.<sup>[96]</sup> The same tendency may be assumed to exist for donors formed by clusters of Mg atoms.

In relation to the discussed topic, we mention the study of the low-temperature exciton luminescence in Si:Mg in ref. [46]. In addition to no-phonon lines that are related to isolated Mg atoms and pairs of atoms, a number of lines with lower emitted photon energies were recorded in spectra. This observation may indicate a variety of magnesium clusters in Si:Mg samples. However, at present, there is no direct relation of these data to shallow Mg-related centers that were observed in ref. [95].

Concluding this part of the review, we can state that magnesium can create a variety of donors in silicon: both single-charge shallow and relatively deep double donors are observed. As is known, the interaction of electromagnetic waves with an impurity is defined by the energy structure of the center, in particular



the spatial localization of its ground state. Quantitative data for the radii of ground states for some donors in silicon were determined in refs. [68,97] from the Zeeman effect spectroscopy at a low temperature. This was done by processing absorption spectra obtained at high magnetic fields within the range of the quadratic Zeeman effect. The data obtained made it possible to quantify the difference in the localization of the electron wave function in the ground state for various donors in silicon, including a number of Mg-related donors.

## 5. Summary and Outlook

Magnesium is ubiquitous in the environment. Demonstrating a high diffusivity in silicon crystals, it can contaminate a semiconductor volume. By giving rise to a number of donor states, along with other rapidly diffusing impurities, the presence of magnesium can change the electrical properties of silicon and influence the operation of electronic devices. At the same time, properties of magnesium impurity in silicon are still not fully understood.

In contrast to elements of V and III groups, which are substitutional impurities in silicon, and which create shallow donor and acceptor levels (each element is characterized by only one type of a donor or acceptor), the presence of magnesium in silicon crystals can give rise to a number of donor states. The best studied is a deep double donor, which is caused by magnesium atoms occupying interstitial positions in the lattice,  $Mg_i$ .

A number of new data on silicon doped with magnesium have been obtained in recent years and were obtained using primarily the sandwich method of the doping silicon. This method enables the preparation of homogeneously doped Si:Mg samples that have a relatively large size, which in turn enables various electrical and optical experiments to be performed.

An interstitial magnesium atom is an example of electrically active helium-like donors in silicon. For such centers, the exchange interaction of electrons defines features in their energy spectra. Compared with other well-known deep double donors in silicon, magnesium in the neutral state is characterized by the maximum value of the exchange interaction. In particular, this predetermines a fundamental interest in studying properties of the “hidden” ortho-states of magnesium impurity in Si as an analog of the helium atom.

Owing to the high chemical activity, magnesium is able to form complexes with a number of other impurities in silicon. As a result, Mg-related donors are observed, whose ionization energies are both lower and higher when compared to the corresponding value for the interstitial  $Mg_i$  center. It was found that the coupling of magnesium with some other impurities, occupying both interstitial (Li) and substitutional (B, Al, Bi, In) positions in the crystal lattice, leads to the formation of shallow donors, the energy structure of which is well described by EMT.

A number of shallow donors, for which the origin could not be interpreted at present as a formation of magnesium complexes with known impurities, were found in the IR absorption spectra of Si:Mg samples, including those obtained by doping a high-purity silicon with Mg. It can be assumed that this class of donors is associated with magnesium clusters, which are characterized by a low electron-binding energy. One can consider an analogy of this phenomenon with the formation of donors in silicon, which

are clusters of chalcogen atoms S, Se, and Te. Depending on the number of atoms in a cluster, these centers can have the electron binding energies in an extended range of values and can be both singly and doubly charged donors. Their nature may also be analogous to the well-known phenomenon of formation of so-called TDs in silicon. In accordance with the existing concept, TDs are electrically active clusters of atoms of another chalcogen (oxygen), which bond with the nearest silicon atoms in various configurations. The number of atoms and their relative positions in a cluster may define the ionization energy of such a complex.

Relatively deep centers with ionization energies close to that for  $Mg_i$ —magnesium–oxygen complex Mg–O and the so-called  $Mg_i^*$  center—are double donors. It may be that some other observed relatively deep centers are also double donors. Possible further studies may include the electronic structure of such helium-like double donors and their structural analysis (bonds in the silicon lattice). From this perspective, the  $Mg_i^*$  center is of special interest because its electronic structure has features that indicate specific lowered symmetry of states. Note that in this connection, the nature of the  $Mg_i^*$  centers can be related to the Mg–Mg pairs, the existence of which was established unambiguously by luminescence experiments on samples prepared from isotopically enriched silicon.

While magnesium in silicon interacts with other impurities, thus forming with them a set of electrically active complexes, one may expect that future studies will reveal complexes that have not yet been observed. It should be noted that because of its ability to create such a large number of impurity-related donors in silicon, magnesium can be placed on a par with oxygen and other chalcogens. As is the case for other rapidly diffusing impurities, magnesium-doped silicon is characterized by a relatively low thermal stability. In particular, even at a low (room) temperature, the diffusion transfer of magnesium in crystals can be observed in the long-term storage of Si:Mg samples. Considering the electronic properties of Mg related centers and the impact of the thermal treatment on its electrical activity, which presently seems not to be quite controllable, Mg is not a dopant whose behavior can be easily controlled in silicon.

Further research may include the study of Czochralski grown silicon doped with Mg; this is a material with a significant oxygen content. Of interest is silicon with a high concentration of defects (in particular, dislocations). Nano- and micro-sized silicon doped with magnesium may also be the subject of a future study.

One of the unsolved problems of Si:Mg is the nature of the electrically inactive component of magnesium in crystals, the amount of which can be several orders of magnitude higher than that in the electrically active state. The data indicate that the high-temperature treatment of silicon-containing Mg suppresses the electrical and optical activity of this impurity. Thus, it can be expected that a small content of magnesium in silicon devices fabricated by the electronic industry, the manufacture of which includes such stages, may not significantly impact the operation of some devices. At the same time, a significant content of magnesium in a neutral form can affect some properties of a semiconductor, e.g., to cause a line broadening in optical transitions of other centers in the crystal. However, a sufficiently high concentration of the electrically active magnesium can be achieved in silicon. Such a material may be of interest in the field of silicon photonics in the IR band. Studies that focused on observing the

IR radiation from Si:Mg samples upon the excitation of crystals may be priority for future research.

## Acknowledgements

The authors thank Prof. V.N. Shastin, Prof. H.-W. Hübers, and Prof. M.L.W. Thewalt, as well as researchers in their groups for the long-term, fruitful collaboration involved in the study of silicon doped with magnesium. The financial support of the work is provided by the Ioffe Institute.

## Conflict of Interest

The authors declare no conflict of interest.

## Keywords

deep and shallow magnesium-related donors, magnesium impurity, silicon

Received: July 7, 2022

Revised: September 13, 2022

Published online: October 27, 2022

- [1] J. Appl. Phys. **2018**, 123 (Issue 16).
- [2] J. Appl. Phys. **2020**, 127 (Issue 19).
- [3] J. C. McCallum, B. C. Johnson, T. Botzem, Appl. Phys. Rev. **2021**, 8, 031314.
- [4] H.-W. Hübers, K. Auen, S. G. Pavlov, E. E. Orlova, R. K. Zhukavin, V. N. Shastin, Appl. Phys. Lett. **1999**, 74, 2655.
- [5] S. G. Pavlov, R. K. Zhukavin, E. E. Orlova, V. N. Shastin, A. V. Kirsanov, H.-W. Hübers, K. Auen, H. Riemann, Phys. Rev. Lett. **2000**, 84, 5220.
- [6] V. N. Shastin, R. K. Zhukavin, E. E. Orlova, S. G. Pavlov, M. H. Rummeli, H.-W. Hübers, J. N. Hovenier, T. O. Klaassen, H. Riemann, V. Bradley, A. F. G. van der Meer, Appl. Phys. Lett. **2002**, 80, 3512.
- [7] S. G. Pavlov, R. K. Zhukavin, V. N. Shastin, H.-W. Hübers, Phys. Status Solidi B **2013**, 250, 9.
- [8] R. F. Franks, J. B. Robertson, Solid State Commun. **1967**, 5, 479.
- [9] L. T. Ho, A. K. Ramdas, Phys. Rev. B **1972**, 5, 462.
- [10] J. E. Baxter, G. Ascarelli, Phys. Rev. **1973**, 7, 2630.
- [11] J. Robertson, R. Franks, Solid State Commun. **1968**, 6, 825.
- [12] R. O. Carlson, Phys. Rev. **1957**, 108, 1390.
- [13] L. T. Ho, Appl. Phys. Lett. **1979**, 35, 409.
- [14] H. G. Grimmeiss, Proc. 17th Int. Conf. on the Physics of Semiconductors, (Eds: J.D. Chadi, W. A. Harrison), Springer, San Francisco, CA, **1984**, p. 589.
- [15] J. Yuan, H. Shen, F. Zhong, X. Deng, Phys. Status Solidi A **2012**, 209, 1002.
- [16] K. J. Morse, R. J. S. Abraham, A. DeAbreu, C. Bowness, T. S. Richards, H. Riemann, N. V. Abrosimov, P. Becker, H.-J. Pohl, M. L. W. Thewalt, S. Simmons, Sci. Adv. **2017**, 3, 1700930.
- [17] H. Riemann, N. V. Abrosimov, N. Nötzel, ECS Transactions **2006**, 3, 53.
- [18] N. V. Abrosimov, N. Nötzel, H. Riemann, K. Irmscher, S. G. Pavlov, H.-W. Hübers, U. Böttger, P. M. Haas, N. Drichko, M. Dressel, Solid State Phenom. **2008**, 131–133, 589.
- [19] B. Pajot, G. Taravella, J. P. Bouchaud, Appl. Phys. Lett. **1973**, 23, 189.
- [20] E. Ohta, M. Sakata, Solid-State Electronics **1979**, 22, 611.
- [21] C. Häßler, G. Pensl, Mater. Sci. Forum **1994**, 143–147, 123.
- [22] K. Matsumoto, Y. Uenaka, Y. Seto, H. Yashiro, H. Nakamura, T. Kimura, T. Uchino, J. Appl. Phys. **2010**, 108, 11370.
- [23] H. Sigmund, J. Electrochem. Soc. **1982**, 129, 2809.
- [24] S. Kawanishi, T. Yoshikawa, Mater. Trans. **2017**, 58, 450.
- [25] H. Sigmund, D. Weiß, in Proc. of the 4th Int. Conf. Ion Implantation: Equipment and Techniques (Eds: H. Ryssel, H. Glawischnig), Springer Series in Electrophysics, Vol. 11, Springer, Berlin, Heidelberg **1983**, p. 473–480.
- [26] H. Francois-Saint-Cyr, E. Anoshkina, F. Stevie, L. Chow, K. Richardson, D. Zhou, J. Vac. Sci. Technol. B **2001**, 19, 1769.
- [27] B. V. King, M. J. Pellin, D. S. Burnett, Appl. Surf. Sci. **2008**, 255, 1454.
- [28] V. M. Arutyunyan, A. P. Akhoyan, Z. N. Adamyan, R. S. Barsegyan, Technical. Phys. **2001**, 46, 198.
- [29] V. B. Shuman, Y. A. Astrov, A. N. Lodygin, L. M. Portsel, Semiconductors **2017**, 51, 1031.
- [30] V. B. Shuman, A. A. Lavrent'ev, Y. A. Astrov, A. N. Lodygin, L. M. Portsel, Semiconductors **2017**, 51, 1.
- [31] Yu. A. Astrov, V. B. Shuman, L. M. Portsel, A. N. Lodygin, S. G. Pavlov, N. V. Abrosimov, V. N. Shastin, H.-W. Hübers, Phys. Status Solidi A **2017**, 214, 1700192.
- [32] A. L. Lin, J. Appl. Phys. **1982**, 53, 6989.
- [33] A. Thilderkvist, M. Kleverman, H. G. Grimmeiss, Phys. Rev. B **1994**, 49, 16338.
- [34] E. A. Steinman, H.-G. Grimmeiss, Semicond. Sci. Technol. **1998**, 13, 329.
- [35] N. Sclar, Prog. Quantum Electron. **1984**, 9, 149.
- [36] X.-Y. Yan, F. Zhang, Y. A. Chang, J. Phase Equilib. **2000**, 21, 379.
- [37] F. Wang, A. M. Matz, O. Tschukin, J. Heimann, B. Mockler, B. Nestler, N. Jost, Adv. Eng. Mater. **2017**, 19, 1700063.
- [38] A. S. Gouralnik, A. M. Maslov, A. Y. Ustinov, S. A. Dotsenko, A. V. Shevlyagin, I. M. Chernev, V. M. Il'yashenko, S. A. Kitan, E. A. Koblova, K. N. Galkin, N. G. Galkin, A. V. Gerasimenko, Appl. Surf. Sci. **2018**, 439, 282.
- [39] V. Seltas, A. Chroneos, F. Vallianatos, J. Mater. Sci. Mater. Electron. **2018**, 29, 12022.
- [40] L. M. Portsel, V. B. Shuman, A. A. Lavrent'ev, A. N. Lodygin, N. V. Abrosimov, Yu. A. Astrov, Semiconductors **2020**, 54, 393.
- [41] A. K. Ramdas, S. Rodriguez, Rep. Prog. Phys. **1981**, 44, 1297.
- [42] A. A. Istratov, H. Hieslmaier, E. R. Weber, Appl. Phys. A **1999**, 69, 13.
- [43] A. A. Istratov, E. R. Weber, J. Electrochem. Soc. **2002**, 149, G21.
- [44] J. Lindroos, D. P. Fenning, D. J. Backlund, E. Verlage, A. Gorgulla, S. K. Estreicher, H. Savin, T. Buonassisi, J. Appl. Phys. **2013**, 113, 204906.
- [45] V. I. Fistul, Decomposition of Supersaturated Semiconductor Solid Solutions, Metallurgia, Moscow **1977** [in Russian].
- [46] R. J. S. Abraham, A. DeAbreu, K. J. Morse, V. B. Shuman, L. M. Portsel, A. N. Lodygin, Yu. A. Astrov, N. V. Abrosimov, S. G. Pavlov, H.-W. Hübers, S. Simmons, M. L. W. Thewalt, Phys. Rev. B **2018**, 98, 205203.
- [47] B. N. Rygalin, A. P. Salmanov, V. P. Pelipas, V. K. Prokofieva, V. V. Batavin, E. B. Sokolov, I. A. Nauk, Neorganicheskiye Mater. **1981**, 17, 1141.
- [48] Yu. A. Astrov, L. M. Portsel, A. N. Lodygin, V. B. Shuman, Semicond. Sci. Technol. **2011**, 26, 055021.
- [49] M. Kleverman, K. Bergman, H.-G. Grimmeiss, Semicond. Sci. Technol. **1986**, 1, 49.
- [50] S. G. Pavlov, N. Deßmann, A. Pohl, V. B. Shuman, L. M. Portsel, A. N. Lodygin, Yu. A. Astrov, S. Winnerl, H. Schneider, N. Stavrias, A. F. G. van der Meer, V. V. Tsyplenkov, K. A. Kovalevsky, R. K. Zhukavin, V. N. Shastin, N. V. Abrosimov, H.-W. Hübers, Phys. Rev. B **2016**, 94, 075208.

- [51] S. G. Pavlov, L. M. Portsel, V. B. Shuman, A. N. Lodygin, Yu. A. Astrov, N. V. Abrosimov, S. A. Lynch, V. V. Tsyplenkov, H.-W. Hübers, *Phys. Rev. Mater.* **2021**, 5, 114607.
- [52] H. Brooks, *Adv. Electron. Electron Phys.* **1955**, 7, 85.
- [53] D. C. Look, *Phys. Rev. B* **1981**, 24, 5852.
- [54] Yu. A. Astrov, L. M. Portsel, V. B. Shuman, A. N. Lodygin, N. V. Abrosimov, S. G. Pavlov, H.-W. Hübers, *Semiconductors* **2021**, 55, 403.
- [55] V. B. Shuman, A. N. Lodygin, L. M. Portsel, A. A. Yakovleva, N. V. Abrosimov, Yu. A. Astrov, *Semiconductors* **2019**, 53, 296.
- [56] S. Froyen, A. Zunger, *Phys. Rev. B* **1986**, 34, 7451.
- [57] *Capacitance Spectroscopy of Semiconductors* (Eds: J. V. Li, G. Ferrari), Pan Stanford Publishing, London **2018**.
- [58] I. V. Antonova, A. V. Vasil'ev, V. I. Panov, S. A. Smagulova, L. S. Smirnov, S. S. Shaimeev, *Sov. Phys. Semicond.* **1987**, 21, 419.
- [59] N. Baber, L. Montelius, M. Kleverman, K. Bergman, H.-G. Grimmeiss, *Phys. Rev. B* **1988**, 38, 10483.
- [60] N. Yarykin, V. B. Shuman, L. M. Portsel, A. N. Lodygin, Yu. A. Astrov, N. V. Abrosimov, J. Weber, *Semiconductors* **2019**, 53, 789.
- [61] L. Dobaczewski, A. R. Peaker, K. Bonde Nielsen, *J. Appl. Phys.* **2004**, 96, 4689.
- [62] L. T. Ho, *Defect Diffusion Forum* **2003**, 221–223, 41.
- [63] L. T. Ho, in *Proc. Joint 30th Inter. Conf. on Infrared and Millimeter Waves and 13th Int. Conf. on Terahertz Electronics*, vol. 1, Terahertz Electronics, Williamsburg, VA, USA, 19–23 September **2005**, p.170–171.
- [64] L. T. Ho, *Phys. B* **2006**, 376–377, 154.
- [65] R. J. S. Abraham, A. DeAbreu, K. J. Morse, V. B. Shuman, L. M. Portsel, A. N. Lodygin, Yu. A. Astrov, N. V. Abrosimov, S. G. Pavlov, H.-W. Hübers, S. Simmons, M. L. W. Thewalt, *Phys. Rev. B* **2018**, 98, 045202.
- [66] N. Yarykin, V. B. Shuman, L. M. Portsel, A. N. Lodygin, Yu. A. Astrov, N. V. Abrosimov, J. Weber, unpublished.
- [67] S. C. Baber, *Thin Solid Films* **1980**, 72, 201.
- [68] S. G. Pavlov, D. L. Kamenskiy, Yu. A. Astrov, V. B. Shuman, L. M. Portsel, A. N. Lodygin, N. V. Abrosimov, H. Engelkamp, A. Marchese, H.-W. Hübers, *Phys. Rev. B* **2020**, 102, 115205.
- [69] C. Jagannath, A. K. Ramdas, *Phys. Rev. B* **1981**, 23, 4426.
- [70] S. M. Kogan, T. M. Lifshits, *Phys. Status Solidi A* **1977**, 39, 11.
- [71] L. V. Berman, S. M. Kogan, *Sov. Physics Semicond.* **1987**, 21, 1537.
- [72] V. N. Shastin, R. K. Zhukavin, K. A. Kovalevsky, V. V. Tsyplenkov, V. V. Rumyantsev, D. V. Shengurov, S. G. Pavlov, V. B. Shuman, L. M. Portsel, A. N. Lodygin, Yu. A. Astrov, N. V. Abrosimov, J. M. Klopff, H.-W. Hübers, *Semiconductors* **2019**, 53, 1234.
- [73] N. A. Bekin, R. K. Zhukavin, V. V. Tsyplenkov, V. N. Shastin, *Proc. of XXV Int. Symp. "Nanophysics & Nanoelectronics"*, Vol. 2, Nizhny Novgorod, Russia, March 09–12 **2021**, p. 580–581.
- [74] W. Kohn, J. M. Luttinger, *Phys. Rev.* **1955**, 98, 915.
- [75] W. Kohn, in *Solid State Physics*, Vol. 5, (Eds: F. Seitz, D. Turnbull), Academic, New York **1957**, p. 257–320.
- [76] P. Wagner, C. Holm, E. Sirtl, R. Oeder, W. Zulehner, in *Advances In Solid State Physics* (Ed: P. Grosse), Vol. 24, Springer, Berlin, Heidelberg **1984**, p. 191–228.
- [77] E. Janzén, R. Stedman, G. Grossmann, H. G. Grimmeiss, *Phys. Rev. B* **1984**, 29, 1907.
- [78] H. G. Grimmeiss, E. Janzén, K. Larsson, *Phys. Rev. B* **1982**, 25, 2627.
- [79] R. E. Peale, K. Muro, A. J. Sievers, F. S. Ham, *Phys. Rev. B* **1988**, 37, 10829.
- [80] R. L. Aggarwal, A. K. Ramdas, *Phys. Rev.* **1965**, 140, A1246.
- [81] K. Bergman, G. Grossmann, H. G. Grimmeiss, M. Stavola, C. Holm, P. Wagner, *Phys. Rev.* **1988**, 37, 10738.
- [82] B. Pajot, *Optical Absorption of Impurities and Defects in Semiconducting Crystal*, Springer Series in Solid-State Sciences, Vol. 158, Springer, Berlin/Heidelberg **2010**.
- [83] S. G. Pavlov, N. V. Abrosimov, V. B. Shuman, L. M. Portsel, A. N. Lodygin, Yu. A. Astrov, R. K. Zhukavin, V. N. Shastin, K. Irmischer, A. Pohl, H.-W. Hübers, *Phys. Status Solidi B* **2019**, 256, 1800514.
- [84] R. J. S. Abraham, V. B. Shuman, L. M. Portsel, A. N. Lodygin, Yu. A. Astrov, N. V. Abrosimov, S. G. Pavlov, H.-W. Hübers, S. Simmons, M. L. W. Thewalt, arXiv:2010.11399, **2020**.
- [85] L. Beinikhes, S. M. Kogan, *Sov. Phys. JETP* **1987**, 66, 164.
- [86] B. A. Andreev, E. B. Kozlov, T. M. Lifshits, *Mater. Sci. Forum* **1995**, 196–201, 121.
- [87] L. T. Ho, A. K. Ramdas, *Phys. Lett. A* **1970**, 32, 23.
- [88] L. T. Ho, F. Y. Lin, W. J. Lin, *Int. J. Infrared Millimeter Waves* **1990**, 14, 1099.
- [89] R. J. S. Abraham, V. B. Shuman, L. M. Portsel, A. N. Lodygin, Yu. A. Astrov, N. V. Abrosimov, S. G. Pavlov, H.-W. Hübers, S. Simmons, M. L. W. Thewalt, *Phys. Rev. B* **2019**, 99, 195207.
- [90] J. R. Haynes, *Phys. Rev. Lett.* **1960**, 4, 361.
- [91] M. O. Henry, E. C. Lightowers, N. Killoran, D. J. Dunstan, B. C. Cavenett, *J. Phys. C: Solid State Phys.* **1981**, 14, L255.
- [92] L. T. Ho, *Phys. Status Solidi B* **1998**, 210, 313.
- [93] L. T. Ho, *Phys. B* **2001**, 302–303, 197.
- [94] P. Pichler, *Intrinsic Point Defects, Impurities, and their Diffusion in Silicon*, Springer, Wien **2004**.
- [95] S. G. Pavlov, Yu. A. Astrov, L. M. Portsel, V. B. Shuman, A. N. Lodygin, N. V. Abrosimov, H.-W. Hübers, *Mater. Sci. Semicond. Process.* **2021**, 130, 105833.
- [96] R. W. Jansen, O. F. Sankey, *Phys. Rev. B* **1986**, 33, 3994.
- [97] J. Li, N. H. Le, K. Litvinenko, S. K. Clowes, H. Engelkamp, S. G. Pavlov, H.-W. Hübers, V. B. Shuman, L. M. Portsel, A. N. Lodygin, Yu. A. Astrov, N. V. Abrosimov, C. R. Pidgeon, A. Fisher, Z. Zeng, Y.-M. Niquet, B. N. Murdin, *Phys. Rev. B* **2018**, 98, 085423.
- [98] G. Grossmann, K. Bergman, M. Kleverman, *Physica* **1987**, 146B, 30.
- [99] K. Bergman, G. Grossmann, H.-G. Grimmeiss, M. Stavola, *Phys. Rev. B* **1986**, 56, 2827.
- [100] E. Rotsaert, P. Clauws, J. Vennik, L. Van Goethem, *J. Appl. Phys.* **1989**, 65, 730.



**Yuri A. Astrov** graduated in 1969 from the Electrotechnical Institute (Leningrad, Russia) with a degree in semiconductor devices. He received his Ph.D. in 1973 and doctor of science in physics and mathematics from the Russian Academy of Sciences in 2005. Since 1973, he has been working at the Ioffe Institute, St. Petersburg, Russia, where he is currently a leading researcher. At present his research interests are mainly related to the study of impurities that form deep levels in silicon.



**Leonid M. Portsel** received his Ph.D. (1984) in physics and mathematics from the Leningrad Polytechnic Institute, Russia. Since 1975, he has been working at the Ioffe Institute, St. Petersburg (Russian Academy of Sciences), and at present holds position of a senior researcher there. His research interests include low-current gas discharges, physics of nonlinear processes, and photoelectric and diffusion phenomena in semiconductors.



**Valentina B. Shuman** received her Physics of Semiconductors diploma in 1957 from the Chernivtsi State University, Chernivtsi, Ukraine, USSR, and Ph.D. in 1966 from the Ioffe Institute (Russian Academy of sciences). Her interests include technology of silicon devices and deep-level impurities in silicon.



**Anatoly N. Lodygin** graduated in 1977 from the Electrotechnical Institute (Leningrad, Russia) with a degree in electronic devices. Since 1981, he has been working at the Ioffe Institute, St. Petersburg (Russian Academy of Sciences), where at present he holds a position of the researcher. His research interest is to study doping silicon with deep impurities and investigate the action of low-current gas-discharge plasma on a semiconductor surface.



**Nikolay V. Abrosimov** received his physics diploma in 1975 from the Nizhny Novgorod State University, Nizhny Novgorod, Russia, and his Ph.D. in solid-state physics in 1984 from the Institute of Solid State Physics of the Russian Academy of Sciences (RAS). Since 1993, he has been holding the position of a senior researcher at the Leibniz-Institut für Kristallzüchtung in Berlin, Germany. His research interests include the crystal growth of both natural and isotopically enriched Si, Ge, and SiGe for basic research and different applications, for example, X-ray and gamma-ray monochromators and MBE targets.